

**A STUDY OF HUMAN BLOOD CELL ADHESION ONTO
CELLULOSE BASED POLYMERS BY DLVO THEORY**

THANEEYA SAMWANG

**A THESIS SUBMITTED IN PARTIAL FULFILLMENT
OF THE REQUIREMENTS FOR
THE DEGREE OF MASTER OF ENGINEERING
(BIOMEDICAL ENGINEERING)
FACULTY OF GRADUATE STUDIES
MAHIDOL UNIVERSITY**

2007

COPYRIGHT OF MAHIDOL UNIVERSITY

Thesis
Entitled

**A STUDY OF HUMAN BLOOD CELL ADHESION ONTO
CELLULOSE BASED POLYMERS BY DLVO THEORY**

.....
Miss. Thaneeya Samwang
Candidate

.....
Asst. Prof. Bovornlak Oonkhanond,
Ph.D. (Chemical Engineering)
Major-Advisor

.....
Prof. Rachanee Udomsangpetch,
Ph.D. (Immunology)
Co-Advisor

.....
Prof. M.R. Jisnuson Svasti, Ph.D.
Dean
Faculty of Graduate Studies

.....
Asst. Prof. Theeraporn Rubcumintara,
Ph.D. (Materials Engineering & Science)
Chair
Master of Engineering Programme in
Biomedical Engineering
Faculty of Engineering

Thesis
Entitled

**A STUDY OF HUMAN BLOOD CELL ADHESION ONTO
CELLULOSE BASED POLYMERS BY DLVO THEORY**

was submitted to the Faculty of Graduate Studies, Mahidol University
For the degree of Master of Engineering (Biomedical Engineering)
on
17 May, 2007

.....
Miss. Thaneeya Samwang
Candidate

.....
Asst. Prof. Theeraporn Rubcumintara,
Ph.D. (Materials Engineering & Science)
Chair

.....
Asst. Prof. Bovornlak Oonkhanond,
Ph.D. (Chemical Engineering)
Member

.....
Prof. Rachanee Udomsangpetch,
Ph.D. (Immunology)
Member

.....
Asst. Prof. Udom Tipayamontri
Ph.D. (Physiology)
Member

.....
Prof. M.R. Jisnuson Svasti, Ph.D.
Dean
Faculty of Graduate Studies
Mahidol University

.....
Asst. Prof. Piya Rattanasuwan,
M. Eng.
Dean
Faculty of Engineering
Mahidol University

ACKNOWLEDGEMENTS

I would like to express my gratitude to my major advisor, Asst. Prof. Dr. Bovornlak Oonkhanond, for his kindness, academic assistance, valuable guidance, encouragement and advice throughout my study. I would like to thank my co-advisers, Prof. Dr. Rachanee Udomsangpetch, for her kindness, constructive supervision, and valuable advices. I would like to thank the advisory committee members, Asst. Prof. Dr. Theeraporn Rubcumintara and Asst. Prof. Dr. Udom Tipayamontri for their kindness and valuable suggestions.

Furthermore, I would like to thank all of the educational service staffs at Chemical Department and Biomedical Engineering Department, Faculty of Engineering, Mahidol University, and the Malaria Research Laboratory, Pathobiology Department, Faculty of Science, Mahidol University for their kind supports.

I would like to sincerely thank to all of my friends for their encouragement. Additionally, I also wish to thank many other people whose names are not mentioned here. Their help in many other ways is also appreciated.

Finally, I would like to thank my mother, Benjaya Samwang, and my father, Pravit Samwang, and everyone in my family whose love and encouragement have supported me.

Thaneeya Samwang

A STUDY OF HUMAN BLOOD CELL ADHESION ONTO CELLULOSE BASED POLYMERS BY DLVO THEORY

THANEEYA SAMWANG 4536775 EGBE/M

M. Eng. (BIOMEDICAL ENGINEERING)

THESIS ADVISORS: BOVORNLAK OONKHANOND, Ph.D.,
RACHANEE UDOMSANGPETCH, Ph.D.**ABSTRACT**

Various polymers have been utilized in clinical medicine including renal dialysis membranes. One of the most popular membranes that has been used is cellulose membrane, which is relatively cheap when compared to synthetic membranes. However, the most important problem of dialysis membrane for patients with renal failure is the white blood cells (WBC) accumulation after exposure to blood. Typically, the number of cells adhering to membranes is governed by the properties of the membrane material. Therefore, this study aims to evaluate the zeta potential of cellulose acetate (CA), cellulose triacetate (CTA) for improving materials in reducing WBC adhesion. The zeta potential of CA, CTA, red blood cell (RBC) and WBC was measured and then the repulsive force and attractive force between CA film/ CTA film and blood cell surface was evaluated based on Derjaguin, Landau, Verwey and Overbeek (DLVO) theory. The study showed that the zeta potential of RBC is highest followed by lymphocytes and neutrophils. The zeta potential of CTA is higher than CA. The summation between repulsive force from zeta potential and attractive force from van der Waal is the energy barrier preventing cell adherence on the material surface. The results show that the strongest energy barrier between neutrophils on CTA film and on CA film at 310 K are 1.509×10^{-16} J and 1.404×10^{-16} J, respectively as compared with other cells. Moreover, the numbers of WBC on the CTA film are less than those on CA film because CTA film represents a higher energy barrier and hydrophobic properties. This study establishes the benefits of CTA as low cost dialysis membrane in blood dialyzer for patients with renal failure.

**KEY WORDS: BLOOD ADHESION/ CELLULOSE MEMBRANE/ DLVO
THEORY/ ZETA POTENTIAL/ INTERACTION FORCE**

68 P.

CONTENTS

	Page
ACKNOWLEDGEMENTS	iii
ABSTRACT	iv
LIST OF TABLES	ix
LIST OF FIGURES	x
LIST OF SYMPOLE AND ABBRIVIATIONS	xiii
CHAPTER	
I INTRODUCTION	1
1. Background	1
2. Problem Statement	4
3. Objectives	5
4. Scope of Study	6
II LITERATURE REVIEW	6
1. Type of Membrane Used in Renal Dialysis Treatment	6
1.1 Cellulose membrane	6
1.2. Cellulose-substituted membrane	7
1.3. Synthetic membrane	7
2. The Adhesions of Human Blood Cells	8
2.1. Blood cells information	8
2.2. The adhesion of blood cells on CA and CTA membranes	11
2.3. Properties of membrane relating cell adhesions	13
2.3.1. Wettability	13
2.3.2. Surface charge	15

CONTENTS (Continued)

		Page
	3. The Interaction Force based on <u>Derjaguin</u> , <u>Landau</u> , <u>Verwey</u> and <u>Overbeek</u> (DLVO) Theory	17
III	METHODOLOGY	22
	1. Materials and Instruments	22
	1.1. Materials and chemical reagents for zeta potential measurement	22
	1.2. Materials and chemical reagents for film fabrication	22
	1.3. Materials and chemical reagents for blood cells incubation	23
	1.4. Instruments	23
	2. Methods	23
	2.1. Zeta potential measurement	24
	2.2. Attractive force and repulsive force calculation	25
	2.3. Cell adhesion test	27
	2.3.1. Film fabrication	27
	2.3.2. Preparation of white blood cells	27
	2.3.3. Cell adhesions test	28
IV	RESULTS	29
	1. Zeta Potential Measurement	29
	2. Interaction Force Calculation	30
	2.1. Attractive force	30
	2.2. Repulsive force	31
	2.3. Net interaction force	33
	3. Cell Adhesion Test	35
	3.1. Surface morphology of films	35
	3.2 Cell adhesion appearances	36

CONTENTS (Continued)

	Page
V DISCUSSION	39
1. Zeta potential measurement and interaction force estimation	39
2. Cell adhesion test	41
3. The relationship between the net interaction forces based on DLVO theory and blood cell adhesions	43
VI CONCLUSION	46
REFERENCES	47
APPENDIX	52
BIOGRAPHY	68

LIST OF TABLES

		Page
Table 2.1	Information of human blood cells	9
Table 2.2	Water contact angle and %DS of SFC and QAC films	14
Table 3.1	Parameters used in DLVO calculation	26
Table 4.1	The SD value of roughness calculated from Image J program	36
Table 4.2	The number of cell differential count from blood with heparin anticoagulant (n=3)	37
Table 4.3	Blood cells adhered on different substrate for incubation period of 1, 2 and 3 hours from OM at x500 magnification	38
Table C1	Compositions of film sample (%w/v)	62
Table D1	Zeta potential measurement of blood cell and polymer in 5%PVP solution at 298 K and 310 K (n=3)	63
Table E1	Maximum net energy barrier between blood cell and CA or CTA substrate at 298 K and 310 K, in case of various cell radius	64
Table E2	Maximum net energy barrier between blood cell and CA or CTA substrate at 298 K and 310 K, in case of same cell radius (radius = 6 μm)	64
Table F1	The number of blood cells ($\times 10^6$ cells/ mm^2) adhered on substrate at 298 K and 310 K for 1, 2 and 3 hour incubation time (n=3)	65
Table F2	The number of neutrophils ($\times 10^6$ cells/ mm^2) adhered on substrate at 298 K and 310K for 1, 2 and 3 hour incubation time (n=3)	66
Table F3	The number of lymphocytes ($\times 10^6$ cells/ mm^2) adhered on substrate at 298 K and 310 K for 1, 2 and 3 hour incubation time(n=3)	66
Table F4	The number of lymphocytes ($\times 10^6$ cells/ mm^2) adhered on substrate at 298 K and 310 K for 1, 2 and 3 hour incubation time	67

LIST OF FIGURES

		Page
Figure 1.1	Scheme of hemodialysis: patient's blood removed and passed into dialyzer for cleaning with controlling pressure	3
Figure 2.1	Cellulose structure derived from cotton	6
Figure 2.2	The structure of cellulose acetate (CA) (left) and cellulose triacetate (CTA) (right): Hydroxyl group of cellulose was replaced with acetate group by acetylation formation and form a new structure of cellulose triacetate	7
Figure 2.3	The temporal variation in the acute inflammatory response, chronic inflammatory response, granulation tissue development, and foreign-body reaction to implanted biomaterials	12
Figure 2.4	A liquid droplet in equilibrium with a horizontal surface. Left: A nonwetting fluid with $90 < \theta < 180$, Right: A wetting fluid with $0 < \theta < 90$	14
Figure 2.5	The picture of stern layer and diffuse electrical double layer	16
Figure 2.6	Schematic diagram of the net interaction is given by the sum of the repulsion force and the van der Waals attractive force	18
Figure 2.7	Total interaction energy curves between bacterial cell and substratum as a function of separation distance. Solid curves represent calculated results based on soft particle analysis. Dashed lines are derived from conventional zeta potentials. Curves from bottom to top are for pH3.75, 4.0, 4.1, 4.5, 5.0 and 7.0, in that order	20
Figure 3.1	Scheme of method overviews	24
Figure 4.1	Zeta potential of CA and CTA polymer in 5% PVP pH 7.4 at 298K and 310K (Bar = SD)	29

LIST OF FIGURES (Continued)

		Page
Figure 4.2	Zeta potential of RBC, neutrophils and lymphocytes in 5% PVP pH 7.4 at 298K and 310K (Bar = SD)	30
Figure 4.3	The attractive force between cellulose substrate and human blood cells composed of RBC, neutrophils and lymphocytes	31
Figure 4.4	The repulsive force between each cell type and both substrates at 298K	31
Figure 4.5	The repulsive force between each cell type and both substrates at 310K	32
Figure 4.6	The repulsive force between each cell type and CA substrate at 298K and 310K	32
Figure 4.7	The repulsive force between each cell type and CTA substrate at 298K and 310K	33
Figure 4.8	The net interaction force between CA and each blood cell type at different temperatures	33
Figure 4.9	The net interaction force between CTA and each blood cell type at different temperatures	34
Figure 4.10	The net interaction force between each substrate and each blood cell type at 298K	34
Figure 4.11	The net interaction force between each substrate and each blood cell type at 310K	35
Figure 4.12	Surface morphology of CA films from OM at x500 magnification at different concentrations (a) CA5 (b) CA10	36
Figure 4.13	Surface morphology of CTA films from OM at x500 magnification at different concentrations (a) CTA5 (b) CTA10	36
Figure 4.14	The mean number of neutrophils, lymphocytes and eosinophils ($\times 10^6$ cells/ mm^2) adhered on different substrates at 1, 2 and 3 hours incubation (Bar = SD, n=3)	37

LIST OF FIGURES (Continued)

		Page
Figure 5.1	White blood cell morphology at x15,000 magnification via SEM	44
Figure B1	The attractive force between cellulose substrate and human blood cells in case of same radius ($a = 6 \times 10^{-6}$ m)	57
Figure B2	The repulsive force between each cells type and CA substrate at 298K and 310K in case of same radius ($a = 6 \times 10^{-6}$ m)	57
Figure B3	The repulsive force between each cells type and CTA substrate at 298 and 310K in case of same radius ($a = 6 \times 10^{-6}$ m)	58
Figure B4	The repulsive force between each cells type and each substrate at 298K in case of same radius ($a = 6 \times 10^{-6}$ m)	58
Figure B5	The repulsive force between each cells type and each substrate at 310K in case of same radius ($a = 6 \times 10^{-6}$ m)	59
Figure B6	The net interaction force between CA and each blood cell type at 289K and 310K in case of same radius ($a = 6 \times 10^{-6}$ m)	59
Figure B7	The net interaction force between CTA and each blood cell type at 289K and 310K in case of same radius ($a = 6 \times 10^{-6}$ m)	60
Figure B8	The net interaction force between each substrate and each blood cell type at 298K temperatures in case of same radius ($a = 6 \times 10^{-6}$ m)	60
Figure B9	The net interaction force between each substrate and each blood cell type at 310K temperatures in case of same radius ($a = 6 \times 10^{-6}$ m)	61

LIST OF SYMBOLS AND ABBREVIATIONS

HD	Hemodialysis
CA	Cellulose acetate
CTA	Cellulose triacetate
PS	Polysulfone
PAN	Polyacrylonitrile
PMMA	Polymethylmethacrylate
PVP	Polyvinylpyrrolidone
vdW	van der Waals
A	Hamaker constant
ζ	Zeta potential
OM	Optical microscope
CRRT	Continuous renal replacement therapy
MW	Molecular weight
WBC	White blood cell
RBC	Red blood cell
μm	Micrometer
$^{\circ}\text{C}$	Celcius (unit of temperature)
K	Kelvin (unit of temperature), $0^{\circ}\text{C} = 273\text{ K}$
mPa·s	MiliPascal-second
CU	Cuprammonium
θ	Contact angle
SFC	Chitosan having N-sulfofurfuryl groups on the surface
FFSA	Chitosan having 5-formyl-2-furan sulfonic acid
QAC	Chitosan having quaternary ammonium groups on the surface
DS	Degree of substitution
ψ	Surface potential

LIST OF SYMBOLS AND ABBREVIATIONS (Continued)

mV	Millivolt
DEAE	Diethylaminoethyl
KCL	Potassium chloride
ATR-FTIR	Attenuated total reflection-fourier transform Infrared spectroscopy
NMR	Nuclear magnetic resonance
DLVO	Derjaguin, Landau, Verwey and Overbeek
V_T	The net interaction force
V_A	van der Waals (vdW) force or attractive force
V_R	Repulsive force
a	Particle radius
H	Separation distance between the plate and sphere
ϵ_0	The permittivity in vacuum = $8.85 \cdot 10^{-12} \text{ C}^2/\text{N} \cdot \text{m}^2$
ϵ_r	The relative dielectric permittivity or dielectric constant of medium
κ	Debye-Hückel parameter
J	Joule
cm	Centimeter
w/v	Weight by volume
CHCl ₃	Chloroform
CH ₃ OH	Methanol
CH ₃ COCH ₃	Acetone
PBS	Phosphate buffer saline
M	Mole
NaCl	Sodium chloride
Na ₂ HPO ₄	Disodium hydrogenphosphate
NaH ₂ PO ₄ ·2H ₂ O	Monosodium phosphate
HCL	Hydrochloric acid
NaHCO ₃	Sodiumhydrogencarbonate

LIST OF SYMBOLS AND ABBREVIATIONS (Continued)

ml	Milliliter
nm	Nanometer = 10^{-9} meter
μ l	Microliter
h	Hour
rpm	Revolutions per Minute
min	Minute
CO ₂	Carbon dioxide
mm	Millimeter
SD	Standard variation
\bar{x}	Mean
n	Total number

CHAPTER I

INTRODUCTION

1. Background

The polymer technologies are growing not only in the field of engineering but also in the field of medicine. Each polymer material has individual properties such as strength, elasticity, degradability and biocompatibility. Especially the biocompatibility of polymer materials should be considered when used in human body. Any materials used in human body or contacted with tissue or human blood could cause the accumulation of blood cells and induce some effects such as inflammatory or allergy the patients. These biological reactions are the immune responses of human. The definition of biocompatibility was defined by William et. al. in 1999 [1] that the biocompatibility means the ability of a material to perform with an appropriate host response in a specific application. The polymer material is usually used to construct artificial organ of the human body such as skin graft, cerebral bone, femoral bone, or artificial kidney due to their inertness. These materials are always contacted with blood especially in the artificial kidney where one side of the polymer membrane is contacted with blood and the other side contacted with dialysate. This process allows the body waste such as urea, creatinine, and excess ions to be removed out of the blood stream so called hemodialysis (HD), which is a method for treating patients with renal failure.

The functions of kidney are important for maintaining the concentration of body fluid and acid-base balance as well as helping to control the blood pressure in our body. Therefore, if the kidney cannot function properly, the body waste products and electrolytes cannot be completely removed and would be accumulated in the blood causing a serious kidney problem such as renal failure disease. Generally, the patients

with renal failure disease can be treated with drugs or hemodialysis depending on the degree of failure. Typically, the hemodialysis treatment is required to a patient who has end-stage renal failure. The main purpose of HD is to restore the composition of the body's fluid environment back to the normal condition. The treatment process occurs by circulating the patient's blood into the dialyzer, which composed of two compartments i.e. blood compartment and the dialysate (a solution of certain minerals and water) compartment. These two compartments are separated with semipermeable porous membrane. The electrolytes in can pass freely through this membrane in both directions until the concentration of the electrolytes in both sides are the same. Therefore, the urea and other waste products in blood can pass through the membrane into the dialysate resulting in the restoration of the electrolyte concentration back to the normal condition. On the other hand, the red blood cells (RBC), white blood cells (WBC), and proteins in the blood is remained in the blood compartment due to their size which are lager than the pore opening of the membrane. The air bubbles and the temperature of the cleaned blood is then removed and adjusted before returning back to the patient as shown in figure 1.1. Normally, hemodialysis requires a blood flow of 400 to 500 ml/min. Therefore, patients require treatment for about 3-4 hours per time to bring back the electrolyte concentration to the body where the number of treatment depends on the degree of failure, typically, three times a week. Another important parameter governed in hemodialysis is the use of heparin as an anticoagulation agent. Heparin is commonly used in blood transfusion process as anticoagulant and anti-platelet agent due to its binding and potent activation of antithrombin III. The concentration of the heparin required for hemodialysis treatment is about 400 to 6,500 IU/hour depending on body weight of patients [2]. This small molecular weight anticoagulant (less than 10,000 Dalton) is then dialyzed through the hemodialysis membrane and leaving tiny amount of heparin in the cleaned blood.

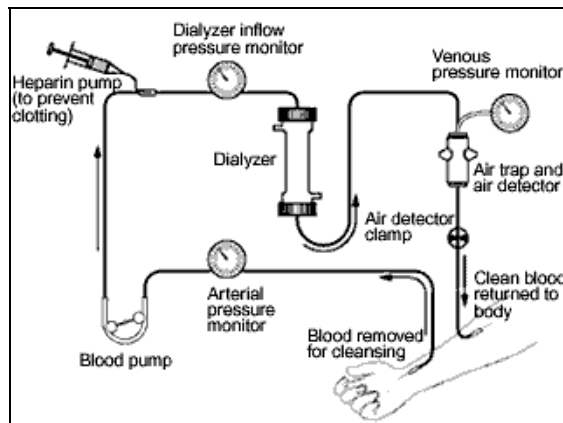


Figure 1.1 Scheme of hemodialysis: patient's blood removed and passed into dialyzer for cleaning with controlling pressure.

The membrane dialyzer can be made of different kinds of materials, which causes the different in their chemical properties, biocompatibility, and blood clot property. The earliest dialysis membrane was derived from cellulose, which comes from wood or plants fiber, so called unmodified cellulose such as cuprophan. This cellulose membrane was then modified by replacing hydroxyl group with acetate group in order to improve the biocompatibility so called modified cellulosic membrane or cellulose-substituted membrane. Some examples of this kind of membrane are hemophan, cellulose acetate (CA) and cellulose triacetate (CTA) membranes. The cellulose acetate was first prepared by Paul Schützenberger in 1865. However, the first chemical extraction of cellulose from wood was manufactured in 1885 by Charles and Edward [3]. The cellulose membranes were used widely for the treatment of renal failure since 1928, when the first human dialysis was performed until about 1960 [4] where the petrochemical and plastic industries were grown rapidly. Thereafter, the use of cellulose membranes was replaced by the synthetics, due to their easier accessibility compare to the cellulose membranes. Although, the synthetic membrane such as polysulfone (PS), polyacrylonitrile (PAN), and polymethylmethacrylate membranes (PMMA) is frequency used in renal dialysis due to their effectiveness of high water permeability and the lower chance to cause the adverse effects to the patients, the cellulose composite membrane is still in used in many hospitals due to its low cost as compared to that of synthesis membrane.

2. Problem Statement

Although, the biocompatibility of hemodialysis membranes are accepted but the accumulating of human blood cells can be found on the membrane surface during the HD process causing the increasing of fouling on membrane surface. This major problem reduces the blood permeation of the membrane which may due to low-hemocompatible surface or a non-specific attachment between cells and material surface. There are some studies reported that the cell accumulation on the membrane surface reduce the transportation of the whole blood in a dialyzer significantly. Usually, the cell accumulation on membrane surface is found to be white blood cells (WBC) especially neutrophils. The study of Wytze et. al. in 1995 [5] showed that the biocompatibility of four HD membrane (Bio-Allegro (hemophan, Cobe/Organon), CA 150 (acetate, Baxter), Acepal 1500 (diacetate, Hospal), and F6 (low-flux polysulfone, Fresenius) are varied greatly causing the loss of white blood cells to the hemodialyzer. This is called leucopenia which referred to the inadequate number of WBC in patient leading to the deficiency of immune function when returned to blood circulation. The similar results were also observed by Hoenich et. al., 2000 [6] and Hiraishi et. al., 2003 [7]. Moreover, several researchers have tried to investigate this problem by focusing in various parameters including surface area, porosity or wettability of membrane. Wytze et. al. [5] found that the maximum percentage of leucocytes loss after passing to a diacetate membrane (55%) is higher than that of hemophan membrane (22%), although, the surface area of diacetate (1.5 m^2) is more than that of hemophan (1 m^2). Additionally, there are several studies that modify surface properties by grafting hydrophilic patches on a hydrophobic matrix to limit the blood–membrane interactions, resulting in the increasing of the blood compatibility such as the study of Deppisch et. al., 1998 [8] and Hoenich et. al., 2000 [9].

Basically, the surface properties of material have played a major role in biomaterial application including surface energy, contact angle, surface tension, electrokinetic of the surface, etc. These interfacial properties affect the interaction force between cells and surface. Kataoka et. al. [10, 11] reported that the interaction of cells with material surfaces consist of two distinct successive stages. The first is an adsorption process in which the interaction is mediated through physicochemical force. The second stage is a metabolism-dependent process, which defined as

adhesion. The adhesion stage occurs by changing the cellular functions as well as in cellular shape leading to a markedly spreading morphology. Therefore, in order to prevent the irreversible function of cell after contacted with a surface. The physicochemical forces at interface between cells and material surface must be studied. This may help us to understand the cells adhesion and prevent the fouling problem later.

Therefore, this study is performed to study the cells adhesion appearances and interest physicochemical force to explain interaction force at interface between cells and membrane surface in order to understand the accumulation of human blood cells on dialysis membrane.

3. Objectives

The purpose of this study is to;

1. Evaluate the significance of surface charge on the adhesion of leucocytes on CA and CTA film using zeta potential measurement.
2. Evaluate the interaction force between leucocytes and CA or CTA substrate based on DLVO theory.
3. Study the adhesion of leucocytes on CA film and on CTA film.

4. Scope of Study

The scope of this study includes;

1. The determination of surface charge on various type of blood cells as well as substrates; neutrophils, lymphocytes, CA and CTA particles by means of zeta potential measurement in polyvinylpyrrolidone (PVP) solution, to mimic the viscosity of the blood.
2. The interaction force estimation based on Derjaguin, Landau, Verwey and Overbeek (DLVO) theory. This approach composed of attractive force from van der Waals (vdW) and repulsive force from double layer repulsion which are dependent on Hamaker constant (A) and zeta potential (ζ) of two surfaces, respectively,.
3. The *in vitro* experiment of cell adhesion on CA and CTA films using neutrophils and lymphocytes. These two membranes are fabricated by solvent casting..

CHAPTER II

LITERATURE REVIEW

1. Type of Membrane Used in Renal Dialysis Treatment

Type of membrane used in dialysis treatment can be divided into three types based on fabricated materials composed of cellulose membrane, cellulose-substituted membrane or modified cellulose membrane, and the last is synthetic membrane.

1.1. Cellulose membrane

Cellulose is the major component of wood or plant fibers such as cotton. Cellulose is a biopolymer made of glucose units $(C_6H_{10}O_5)_n$ linkage in a linear chain formation. Each unit of cellulose, which is D-(+)-glucose unit was joined by a glycoside linkage to C-4 of the next, as shown in figure 2.1 and this chain can be broken by action of acid. This cellulose is water insoluble polymer, therefore, the hydraulic permeability of cellulose is relatively low resulting in low flux permeation of liquid water to this membrane. The advantage of this membrane is it has a molecular weight cutoff at about 2000 Dalton, which is good preventing the loss of large molecular size as albumin (68,000 Dalton). However, this type of membrane is not widely used because it causes the decreasing of white blood cells (WBC) after passed membrane as compared modified cellulose membranes or synthetic membrane [12] so called poor biocompatibility.

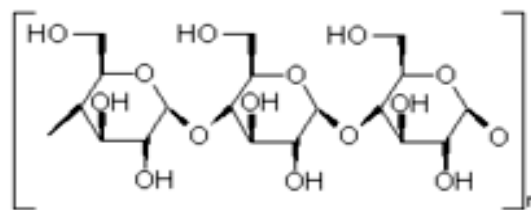


Figure 2.1 Cellulose structure derived from cotton

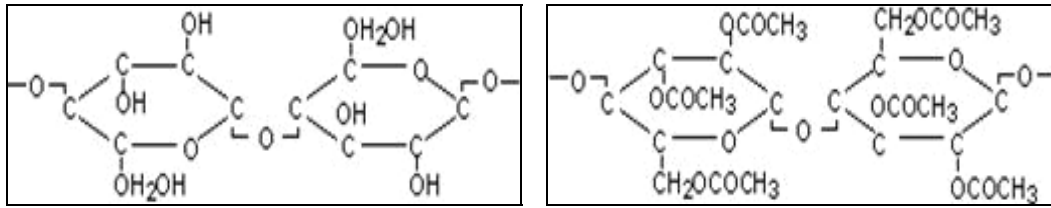


Figure 2.2 The structure of CA (left) and CTA (right): Hydroxyl group of cellulose was replaced with acetate group by acetylation formation and form a new structure of CTA

1.2. Cellulose-substituted membrane (or modified cellulose membrane)

This type is cellulose, which hydroxyl group (-OH) of D-glucose is substituted with other groups such as acetic anhydride, acetic acid, and sulfuric acid. The substituted cellulose membrane was developed and widely used in various industries i.e. textiles, films, and various plastic objects including medical applications such as hemodialysis [13]. Cellulose acetate membrane (CA) is widely used in renal dialysis therapy due to its better biocompatibility compared to the nature cellulose membrane. This type of membrane is also ease to perform porous structure by solvent casting method as compared with other types of substituted cellulose membrane. Typically, the degree substitution of hydroxyl group in cellulose structure determines the quality of the cellulose membrane. If the hydroxyl group substitution is greater than 92 percent, the modified cellulose polymer is then called cellulose triacetate (CTA). This was assigned by Federal Trade Commission definition [14]. However, if the substitution degree less than 92 percent this cellulose is called cellulose diacetate. The different degree of hydroxyl substitution in cellulose also affects the hydrophilic property of the membrane due to the lack of OH group in the molecule (see figure 2.2). Normally, CTA shows a lower hydrophilic property than that of CA resulting in a higher resistance to fouling compared with CA. Moreover, the CTA membrane is considered to be cheaper compared to the synthetic membranes such as polysulfone (PS). Thus, CTA membrane is more preferred for using as hemodialysis membrane.

1.3. Synthetic membrane

Typically, synthetic membranes can be prepared from engineered thermoplastics such as polymethylmethacrylate (PMMA), polyacrylonitrile (PAN), and polysulfone (PS). These materials are naturally hydrophobic and require blending

with hydrophilic polymers to perform porous structure. The formation of asymmetric and anisotropic structures of synthetic membrane is easily prepared by changing composite, which leads to high water permeability property.

Although, the synthetic membrane was modified to be compatible to use in renal dialysis, the blood cells accumulation on the membrane surface is still present. Therefore, the cellulose triacetate membrane is more preferred due to the low cost. Recently, Pichaiwong et. al. [15] studied the clearance performances between the cellulose triacetate membrane (CTA, Sureflux150E) and the standard synthetic membrane (PS, AV-400) in continuous renal replacement therapy (CRRT). It is found that the creatine (MW ~ 113.14), uric acid (MW ~ 168.11) and albumin (MW ~ 68,000) clearance of CTA membrane (Sureflux150E) is not significantly different from the polysulfone membrane (AV-400). This result suggested that the use of CTA membrane in patients with renal failure could provide comparable efficacy with the standard synthetic membrane such as PS.

2. The Adhesions of Human Blood Cells

2.1. Blood cells information

The composition of a whole blood is consisted of 46-63 % of a fluid connective tissue with an extracellular matrix called plasma and 37-54 % of formed elements. Plasma consists of plasma protein, other solutes, and water. Protein dissolved in plasma, there are three primaries classed of plasma proteins that is albumin, globulins and fibrinogen. The main function of plasma protein is to prevent them from crossing capillary walls. Albumin is the most abundant plasma protein, constitute about 60 % of the plasma proteins. The formed element is consisted of red blood cell (RBC) so called erythrocyte and white blood cell (WBC) so called leukocytes. Beside the cellular component, there is a class of non-cellular formed element that is platelets. The briefly information and morphology of each blood cell is illustrated in table 2.1.

Table 2.1 Information of blood cells [16]



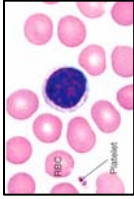
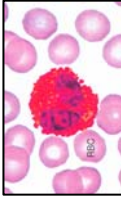
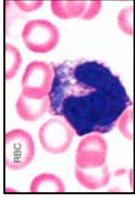
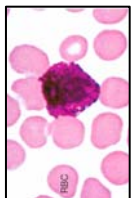
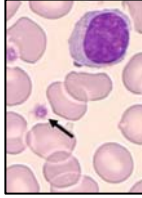
Type of cells	Descriptions	Picture [16]
Red blood cells (RBC)	<p>RBC typically circulate at 5×10^6 cells per μl and may composed of 40-45% of the total blood volume. Radius of RBC is about 7 μm. RBC has no nucleus because nucleus is extruded from the cell as it matures. They contain protein chemical called hemoglobin which is bright red in color. Hemoglobin contains the element Iron, making it an excellent vehicle for transporting oxygen and carbon dioxide.</p>	
Neutrophils	<p>Neutrophils are the most numerous WBC. There is about 50-70% of all WBC. Radius of neutrophil is about 10-15 μm. Nucleus of neutrophil has 2-5 lobes. The neutrophils are mature cells that can attack and destroy foreign particles such as bacteria and viruses even in the circulating blood by project pseudopodia in all directions around the particles.</p>	
Lymphocytes	<p>There is about 20-30% of all WBC. General, lymphocytes can be divided into two kinds i.e. small lymphocyte and large lymphocyte. Radius of small lymphocyte is about 6-9 μm and of large lymphocyte is about 17-30 μm. Lymphocytes are responsible for specific recognition such as viruses, cancer cells, and other foreign substances.</p>	
Eosinophils	<p>There is about 0-7% of all WBC and are about 10-20 micrometers in size. Eosinophils are a type of white blood cell that are responsible for combating infection by parasites in the body and functions in inflammatory reactions including allergy and asthma</p>	

Table 2.1 Information of blood cells (continued)

Type of cells	Descriptions	Picture [16]
Monocytes	<p>There are 1.7-9% of all white blood cells. Radius of monocyte is about 2-6 time of RBC. Monocyte can mobile in the bloodstream or in body tissues where they mature to cells called Macrophages. Monocytes capture and destroy bacteria and other foreign substances, remove dead cells from the body, participate in iron metabolism, and process information about foreign antigens for the lymphocytes.</p>	
Bosophils	<p>There are less than 1% of all white blood cells. Basophils can secrete high concentrations of heparin and histamine in their granules, which significant play an important role in enhancing inflammatory reaction.</p>	
Platelets	<p>Platelets are also known as thrombocytes. Platelets are nonnucleated, disk-shaped cells having 3-4 μm of diameter and circulate at about 250,000 cells per μl. They are small fragments of cells that clump together and stick to inner surface of blood vessels to plug up leaks. The platelets release a substance for clotting of blood. The platelets cause the injured site to shrink and seal off.</p>	

The properties of the whole blood [16] are

a. *Temperature*: Blood temperature is 37°C , the changing of temperature has influence on the protein deformation, function and blood viscosity.

b. *Viscosity*: Blood viscosity is about $30\text{ mPa}\cdot\text{s}$ which is five times greater than that of water since it is composed of plasma, dissolved proteins and several formed element such as red blood cells. Blood viscosity can be determined using viscometers which is strongly dependent on temperature. Cinar et. al. [17] explained the relation between temperature and viscosity using capillary tube viscometer method by decreasing temperature from 36.5°C to 22°C , blood viscosity increased 26.13% resulting in decreasing blood flow rate.

c. *pH*: Blood pH is in the range of 7.35 to 7.45 with the averages pH of 7.4. By varying blood pH over the normal range, cells can be disrupted by breaking chemical bonds and changing the shapes of complex molecules.

2.2 The adhesion of blood cells on CA and CTA membranes

General, when artificial material exposes to blood, this contacting results in the activation of immune system, which divided into two components i.e. innate immune system and adaptive immune system. Adaptive immune system is composed of highly specialized, systemic cells and processes that eliminate pathogenic challenges. The adaptive or "specific" immune system is activated by the non-specific and evolutionarily older innate immune system. The innate immune system is a dominant system of host defense, which comprises the cells and mechanisms that defend the host from infection by other organisms in a generic way [18]. Another function of innate immune system is inflammation, which is stimulated by chemical factors released by injured cells. Chemical factors activates the phagocytic cell especially neutrophils. Neutrophils are the most abundant type of phagocyte, normally representing 50 to 60% of the total circulating leukocytes, and are usually the first cells to arrive at the scene of infection. The response of cells is established in figure 2.3.

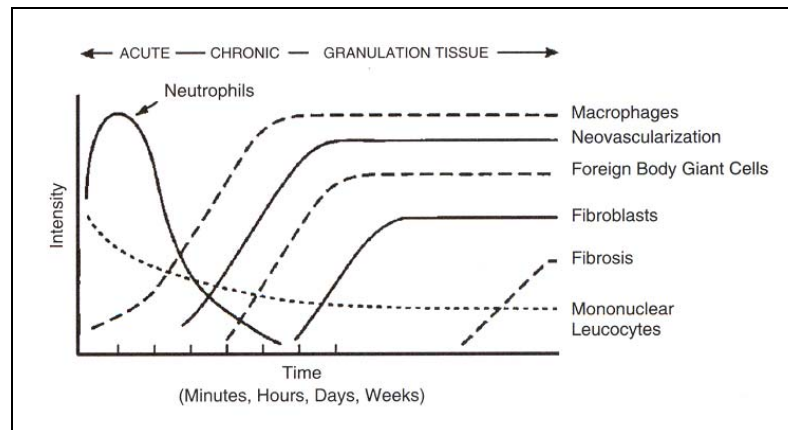


Figure 2.3 The temporal variation in the acute inflammatory response, chronic inflammatory response, granulation tissue development, and foreign-body reaction to implanted biomaterials [19]

Furthermore, material contacting blood involves a complex response between the material surface and circulating blood platelets and blood proteins especially coagulation enzymes [20]. In a stable state, platelets are smooth and discoid in shape but they are easily activated from contacting foreign body causing platelet to become sticky and secrete granule contents. This activated the formation of a blood clot or thrombus that may obstruct blood flow [21]. However, the immune system can be activated depending on several factors such as type of materials, surface properties, and the biologic environment.

Additionally, several researches have reviewed that types of membrane have influence on the adhesion of those cells by observing from the number of cells after passed dialysis membrane. For example in a study of Falkenhagen et. al. [22], seven different types of dialysers were investigated. This study was carried out in five dialysis centers in four countries. The behaviors of white blood cells and the complement system were monitored. The results showed that cuprammonium cellulose membranes (G10-3N and G120 M) have the largest changes in the number of white blood cells (monocytes and neutrophils) after passing in the dialysers. The dialysers made of cellulose acetate and polysulphone membranes (Duo-Flux Artificial Kidney, CD 4000, and F60) produced only a moderate decreasing of the number of WBC, composed of neutrophils, lymphocytes and monocytes. Then Grooteman et. al. [23] investigated the influence of hemodialysis (HD) membrane on lymphocytes. The

commercial dialyzers, which were used in their experiment, were CTA, cuprammonium (CU) and PS dialyzer. Their experiments were performed for testing in patients. The total number of leukocyte count, differentiation of lymphocyte, lymphocyte subpopulations and activation status in peripheral blood were analyzed after 30 and 180 minutes of HD using flow cytometer. The dialyser eluates were also collected after disconnecting the extracorporeal circuit from patients and recirculating with PBS containing EDTA for 20 minutes. They reported that only CU dialysers induced a significant drop in the number of leucocytes in peripheral blood after 30 minutes of HD process. However, the majority types of the cells found in eluates was PMN, which could be found on every type of the dialyzer. The cells number in eluate solution of CA is more than other type. This study was concluded that the CU dialyser cause the greatest loss of leucocytes compared to the others. Moreover, the cells attached on the CU dialyser are difficult to elute with PBS as compared to the others. This study was also established the effectiveness of each membrane type in blood dialysis by observing the blood cells numbers after blood exposed to a dialysis membrane. The results represented that the different type of membrane leading to the different type of cells attached on the surface. This information was very useful for evaluating blood compatibility for each type of membranes.

Nevertheless, the particular blood response to materials is not well-established or predictable may due to the complexity of material properties in terms of geometry and composition. There are several researches try to resolve blood cell adhesion problem by focusing on the material properties i.e. wettability (hydrophilic/hydrophobic properties) and surface charge.

2.3. Properties of membrane relating cell adhesions

2.3.1. Wettability

Wettability of surface is usually determined by the contact angle (θ) between a liquid droplet on horizontal surface and usually referred as the effective of water adsorption on surface [24]. The wettability may be represented in term the hydrophilic/ hydrophobic properties of material surface. Contact angle is depended on the type of surface and liquid, which led to the variation of angle as shown in figure 2.4. The surface is defined as non wetting when angle is greater than 90° (left figure), On the other hand, this surface is called wetting when contact angle is less than 90° .

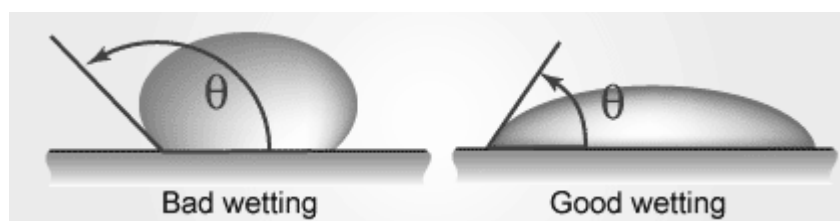


Figure 2.4 A liquid droplet in equilibrium with a horizontal surface. Left: A nonwetting fluid with $90 < \theta < 180$, Right: A wetting fluid with $0 < \theta < 90$ [25]

Voravee et. al. [26] studied the effect of the alternated functional group on chitosan film composites to the wettability of the surfaces. This includes chitosan containing N-sulfofurfuryl groups (SFC), chitosan containing 5-formyl-2-furan sulfonic acid (FFSA), and chitosan containing quaternary ammonium groups on the surface (QAC). The effects of degree substitution (DS) of SFC, FFSA and QAC films to the contact angle were studied and shown in table 2.2. The results show that a higher degree of N-sulfofurfuryl group substitution on chitosan (S1 to S3) led to a lower water contact angle. This indicates that the increasing of N-sulfofurfuryl groups leading to the reducing of hydrophilicity.

Table 2.2 Water contact angle and %DS of SFC and QAC films

Samples	% DS	Water contact angle
Chitosan film	-	79.6 ± 1.1
SFC film (S1)	3.0	71.2 ± 2.6
SFC film (S2)	4.4	67.8 ± 3.8
SFC film (S3)	7.7	62.0 ± 1.9
QAC film (Q1)	N/A	74.2 ± 2.2
QAC film (Q2)	0.5	63.2 ± 3.6
QAC film (Q3)	5	61.0 ± 1.7

2.3.2. Surface charge

Typically, the surface charge can be represented by zeta potential. The colloidal particles dispersed in an electrolyte solution are electrically charged due to their ionic characteristics and dipolar attribution. Those particles are surrounded by oppositely charged ions and form a layer so called stern layer. Outside this layer, there are varying compositions of ions of opposite polarities forming a cloud-like so called diffuse electrical double layer [27]. The thickness of this layer depends on the opposite ion in solution, as shown in figure 2.5. The double layer causes an electrokinetic potential between the surfaces of the colloid. This potential difference is on the order of millivolts (mV) and is referred to as the surface potential (Ψ), which related to the surface charge and the thickness of double layer. By applying some potential across the system containing charged particles in a media, the colloid particles will move to opposite polarities with a fixed velocity. When a particle moved in the media, a boundary called slip plane appears between the moving particles and media, which occur at the interface between stern layer and electrical double layer. There is an electrical potential occurred at this interface is called zeta potential (ζ), which always defined as surface charge so called surface potential.

The velocity of charged particle is obtained through Stoke's law [28], which is written as

$$F = 6\pi\mu r v \quad (1)$$

where F is force, μ is viscosity of medium, r is particle radius, and v is velocity of particle. Then ζ can be evaluated from Helmholtz theory written as

$$v = \frac{\varepsilon E \zeta}{6\pi\mu} \quad (2)$$

where ε is dielectric constant of medium, E is electric field and ζ is zeta potential, which is proportional to the velocity of particle.

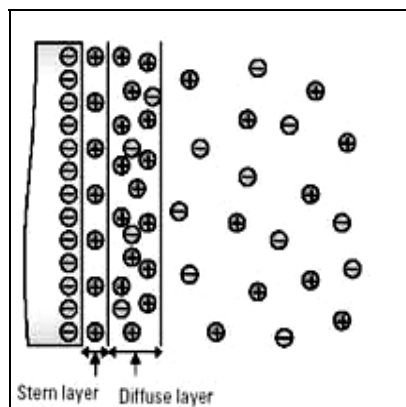


Figure 2.5 The picture of stern layer and diffuse electrical double layer [29]

Warner et. al. [30] showed the relation between zeta potential of polymer and functional group on polymer. They measured zeta potential of flat HD membrane i.e. polysulfone (F60), cellulose (CuprophaneTM) and diethylaminoethyl (DEAE)-cellulose (a modified cellulose) from streaming potential measurements (Electrokinetic Analyzer EKA, A. Paar BmbH) in potassium chloride (KCl) solutions. In case of cellulose based membrane, maximum value of zeta potential of modified cellulose is higher than that of unmodified cellulose. This zeta potential is correspond to percentage of amine surface sites.

Additionally, Voravee et. al. [26] studied the effect of the alternated functional group on chitosan film surface composed of SFC film, FFSA film and QAC film (detail is described in past topic). The characteristics of those samples were studied by ATR-FTIR, NMR, contact angle and zeta-potential measurements. From zeta potential measurement, the QAC film possessed positive zeta potential of +5.5 whereas the SFC exhibited negative zeta potential of -22.2 as compared to -13.1 mV of chitosan. This suggested that the changing of functional group not only influence on contact angle but also zeta potential of each material. The different in percentage of –OH substitution on CA and CTA, the zeta potential of CA and CTA should be different. The different value of zeta potential may lead to the different of number of cells on surfaces.

3. The Interaction Force based on Derjaguin, Landau, Verwey and Overbeek (DLVO) Theory

DLVO theory is the quantitative theory, which was developed by Derjaguin, Landau, Verwey and Overbeek in 1940s [31] to describe the net interaction force (V_T) between charged surfaces interacting through a liquid medium. This interaction can be calculated from the balance of van der Waals (vdW) force (V_A), which is a weak attractive force between atoms or dipolar molecules, and electrostatic double layer or repulsive force (V_R), which occurs from the overlapping of electrical double layer of two particles, which have differential surface potential.

The characteristic of summary force explained by this theory is shown in figure 2.6. The energy barrier resulting from the repulsive force prevents two particles approaching one another and adhering together. However, if the particles collide with sufficient energy to overcome that barrier, the attractive force will pull them into contact where they adhere strongly and irreversibly together. Therefore if the particles have a sufficiently high repulsion, the dispersion will resist flocculation and the colloidal system will be stable. However if a repulsion mechanism does not exist then flocculation or coagulation will eventually take place.

Hermansson et. al. [32] explained the adhesion of microorganisms using DLVO theory. The summation of attraction and repulsion forces yield the total interaction force showed in equation (3)

$$V_T = V_A + V_R \quad (3)$$

where, V_T is the net interaction. V_A is vdW force or called attractive force, which leads to the aggregation of particles and V_R is repulsive force, which will be large approached when there is overlap in electrical double layers between two particles preventing aggregation of particles.

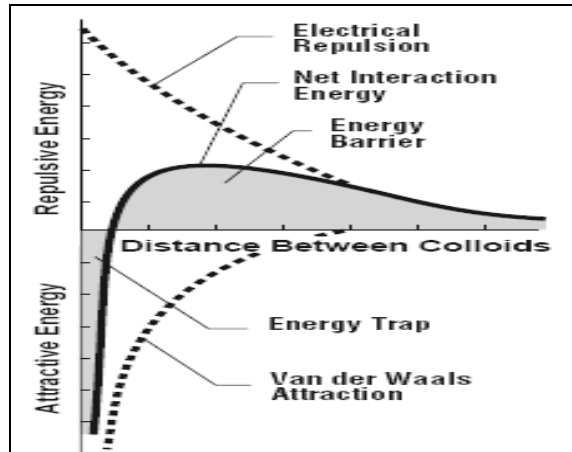


Figure 2.6 Schematic diagram of the net interaction is given by the sum of the double layer repulsion and the van der Waals attractive forces [33].

V_A can be expressed as a function of the Hamaker constant (A). The Hamaker constant of particle can be calculated from Lifshitz theory if the dielectric constant (ϵ) of the surfaces within the interacting medium are accurately known. In the study of Bergström et. al. in 1999 [34], the Hamaker constant of cellulose film were evaluated from spectroscopic ellipsometric measurements and reviewed that $A = 58$ zJ in air and 8.0 zJ in water. The dielectric constant (ϵ) used in their study was 7 ± 1 for both regenerated cellulose and cellulose film.

Attractive force was calculated depending on surface geometry of particles, in case of the interaction between a plate surface and a sphere, V_A was derived by Lyklema et. al. [35] and can be written as

$$V_A = -\frac{A_{12/3}}{6} \frac{[2a(H+a)]}{H(H+2a)} + \ln \frac{H}{H+2a} \tag{4}$$

$$A_{12/3} = \sqrt{A_{11/3} \cdot A_{22/3}} \tag{5}$$

where a is particle radius, H is the separation distance between the plate and sphere particle. $A_{12/3}$ is the Hamaker constant for the vdW interaction of particle 1 and substrate 2 in liquid 3. This equation can be assumed that while H is stable and a is increased, V_A will be increased. By maintaining a constant and decreasing H , this lead

to the occurring of V_A due to there is repulsive force reduction as shown in figure 2.6. If two surfaces approaching together the repulsive force increased due to the strong repulsion from double layer on the two surfaces until the maximum repulsion is achieved. At this position the interaction force required to move these two surfaces to this distance is determined as the energy barrier. After that the repulsion force decreased rapidly due to the strong attraction until two surfaces are attached.

Derjaguin and Landau [36] derived the repulsion interaction as a function of the distance between two surfaces (H). Hogg et. al. [37] further derived and provided an expression for the case of the interaction between a sphere and a plate by assuming that one sphere surface has a very large diameter compared to the other. This assumption allowed us to imagine that the large particle behave like flat surface relatively to the small sphere. The repulsion force between plate and sphere can then be written as

$$V_R = \pi \varepsilon_r \varepsilon_0 a \left[(\psi_1^2 + \psi_2^2) \ln \left(\frac{\exp(2\kappa H_0) - 1}{\exp(2\kappa H)} \right) + 2\psi_1 \psi_2 \ln \left(\frac{\exp(\kappa H_0) + 1}{\exp(\kappa H) - 1} \right) \right] \quad (6)$$

where ε_0 is the permittivity in vacuum, is defined to have the numerical value of $\varepsilon_0 = 8.85 \cdot 10^{-12} \text{ C}^2/\text{N}\cdot\text{m}^2$. ε_r is the relative dielectric permittivity or dielectric constant of medium. κ is Debye-Hückel parameter, H_0 is the shortest distance between the spherical surface and plate surface. ψ_1 , ψ_2 are the surface potentials of the sphere and the plate, respectively. However, if zeta potentials of sphere and plate are measured in the same solution, ε_r , ε_0 and κ are constant, V_R will be varied depending on zeta potential of each subject.

The net interaction force based on DLVO theory between sphere and plate can be calculated from summary equation of (4) and (6). The net interaction force versus distance between two surfaces can be plotted as shown in figure 2.6.

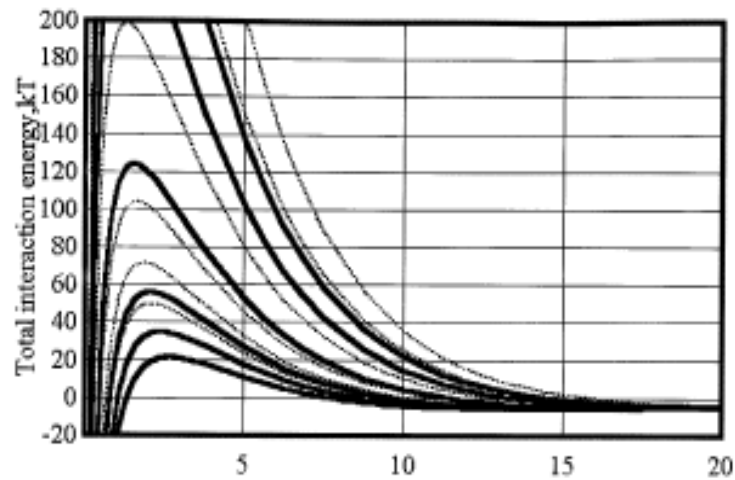


Figure 2.7 Total interaction energy curves between bacterial cell and substratum as a function of separation distance. Solid curves represent calculated results based on soft particle analysis. Dashed lines are derived from conventional zeta potentials. Curves from bottom to top are for pH 3.75, 4.0, 4.1, 4.5, 5.0 and 7.0, in that order [38].

Although the early application of DLVO theory was to account for the behavior of colloid suspensions but from a study Hayashi et. al. in 2001 [38], they showed that the DLVO theory can be applied to bacterial and glass surface system. Zeta potentials of these two materials were determined by Electrophoretic mobility measurement based on Smoluchowski theory. The cell radius of $0.5 \mu\text{m}$, Hamaker constant of $6.41 \times 10^{-21} \text{ J}$, and ionic strength of 0.01 M were used for the estimation. Additionally, bacterial adhesion was studied by feeding bacterial suspension (about $5 \times 10^8 \text{ cell/ cm}^3$) into packed column containing 10g of glass beads. The result by varying pH of the medium showed that cell adhesion was promoted to substratum when pH decreased. This was suggested by the authors that the cell adhesion was increased because the reduction of electro-repulsive force as shown in the total interaction energy plots in figure 2.7.

Kataoka et. al. [10, 11] suggested that the interaction of cells with material surfaces consist of two distinct successive stages. The primary stage is an adsorption process, which is mediated through physicochemical force composing of attractive force and repulsive force. The second stage is a metabolism-dependent process, which defined as “adhesion stage”. In the process of adhesion step, the change of cellular

functions as well as in cellular shape leads to a markedly spreading of cell morphology. This represented that the blood cells adhered on membrane surface was influenced from attractive force and electrostatic repulsion force [32, 38, 39]. Furthermore, to improve the understanding about blood cells adhesion at the primary stage, DLVO theory is a suitable method for explaining the repulsive force occurring between blood cells and CA or CTA film surface using the zeta potential at same condition with cell adhesion test.

CHAPTER III

METHODOLOGY

1. Materials and Instruments

1.1. Materials and chemical reagents for zeta potential measurement

- Cellulose acetate (CA) (Fluka, Switzerland) and cellulose triacetate (CTA) polymer (Fluka, Switzerland)
- Neutrophil, lymphocyte and red blood cell (RBC)
- Lymphoprep solution
- Polymorprep solution
- RPMI 1640 medium (GIBCO BRL, USA)
- 5% polyvinylpyrrolidone (PVP) (Sigma, USA): 5 g of PVP powder dissolved in 100 ml of 0.01M phosphate buffer saline (PBS). PVP solution was used for zeta potential measurement because it have used in the study of RBC rheology, PVP solution is homogeneous liquid, which no have large protein molecules like as PBS solution preventing cells damage or disturbing detection during cells flow in aperture.
- 0.01M PBS: 8.5 g sodium chloride (NaCl), 1.35 g disodium hydrogenphosphat (Na_2HPO_4) and 3.9 g monosodium phosphate ($\text{NaH}_2\text{PO}_4 \cdot 2\text{H}_2\text{O}$) dissolved in 1000 ml of distilled water.

1.2. Materials and chemical reagents for film fabrication

- CA and CTA polymer
- Chloroform (CHCl_3) (BDH, UK)
- Acetone (BDH, UK)
- Methanol (CH_3OH) (BDH, UK)
- Acetic acid (CH_3COCH_3) (BDH, UK)
- DI water

1.3. Materials and chemical reagents for blood cells incubation

- Whole blood donated from healthy Thai donor was collected in heparin tube, which prepared at Malaria Research Laboratory, Pathobiology Department, Faculty of Science, Mahidol University.
- McCoy's medium (GIBCO BRL, USA)
- 0.01M PBS
- Distilled water
- Petri-dish and forceps

1.4. Instruments

- Optical microscope (Olympus, USA)
- Zetasizer 3000 (Malvern, UK)

2. Methods

There are two parts of this experiment. The first part composed of zeta potential measurement and force calculation. The quantitative attractive force from Hamaker constant and repulsive force from zeta potential measurement calculated from DLVO theory is evaluated. The second part in this study composed of the cellulose substrate film fabrication and the cells adhesion on the different types of cellulose composite films. The films are prepared using cellulose acetate and cellulose triacetate at two concentrations. The experiment procedure is shown in figure 3.1.

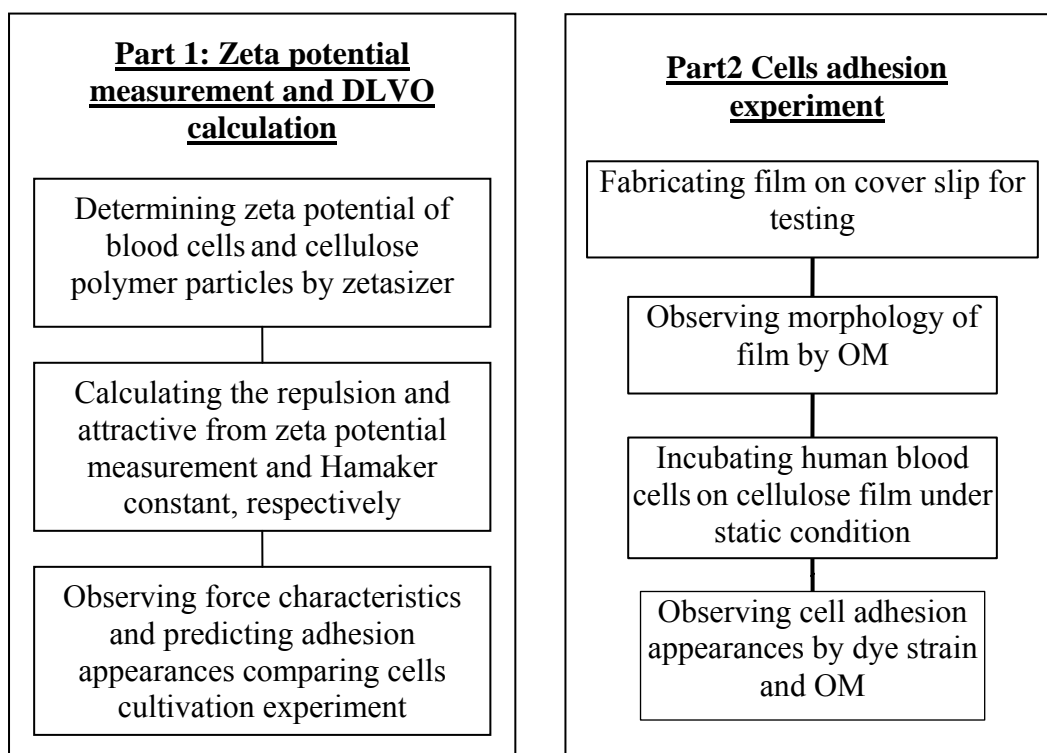


Figure 3.1 Scheme of method overviews

2.1. Zeta potential measurement

Zeta potential (ζ) of blood cells composed of neutrophils, lymphocytes and red blood cells and of CA and CTA polymer is measured from zetasizer 3000 instrument. Cellulose polymer particle and blood cells is dispersed in PVP solution with viscosity of 30 mPa·s. The dielectical constant of cellulose polymer is 76.175. The pH of PVP is adjusted with 0.1M HCL and 1 M NaHCO₃ to have the pH of 7.4.

Lymphocytes separation method

The human blood from healthy donor is collected into a tube with heparin as the anticoagulant. The medium is added into the blood tube in the twice volume of that of original blood. The blood samples and Lymphoprep solution are maintained at 4 °C during centrifugation and storing through out the entire study. The 5.0 ml of anticoagulated blood is carefully layered over 3.0 ml of Lymphoprep solution in a 12 ml centrifuge tube. This process must be carried out carefully to avoid the mixing of the blood with the separation fluid. The samples layered over Lymphoprep solution is then centrifuged for 800 x g for 20 minutes at 4°C. After centrifugation, lymphocyte cells layer should be visible and is then separated using a

pasteur pipette into new a centrifugal tube filling with RPMI medium or 1xPBS. The washing process by centrifugation is carried out twice to remove Lymphoprep solution before further utilization. The centrifugation is carried out at 2,500 rpm for 10 minutes while maintaining the temperature at 4⁰C. After that, the lymphocyte cells are counted by hemocytometer. Then cells are separated in 10 ml 5%PVP solution about 0.5-0.8 x10⁶ cells/ml for zeta potential determination. Formula of blood cell counting by hemocytometer is calculated as follows

$$\frac{\text{Total number of cells in 4 windows}}{4} \times \text{dilution factor} \times 10^4 = \underline{Y} \text{ cells per ml}$$

$$\underline{Y} \times \text{volume of solution} = \text{total number of cells per ml.}$$

PMN (Neutrophils) separation method

The human blood from healthy donor is collected into a tube with heparin as an anticoagulant. The medium is added into the blood tube in the twice volume of that of original blood. The blood samples and the Polymorphprep solution is maintain at the temperature of 18-22 ⁰C through out the process. The 5.0 ml of anticoagulated blood is carefully layered over 3.0 ml of Polymorphprep solution in a 12 ml centrifuge tube and avoid mixing of the blood with the separation fluid. The samples layered over Polymorphprep solution is centrifuged for 500 x g for 30 minutes at 18-22 ⁰C. After centrifugation, two leukocyte layers should be visible. The top layer consists of mononuclear cells and the lower layer consists of neutrophils cells. The cells are then transferred using a Pasteur pipette into a new centrifuge tube. The centrifugation is carried twice to remove Polymorphprep solution before further use. The centrifuge conditions are 2,500 rpm for 10 minutes at 18-22 ⁰C. The lymphocyte cells are then counted using hemocytometer. Then cells are separated in 10 ml 5%PVP solution about 0.5-0.8 x10⁶ cells/ml for zeta potential measurement.

2.2. Attractive force and repulsive force calculation

The interaction force between cell and cellulose based polymer (CA and CTA) are estimated based on the assumption that all cells are spheres and the cellulose

substrate are flat smooth surfaces. The equation of attractive force and repulsion force used in this study follows Lyklema et. al. [35] and Hogg et. al. [37] respectively;

$$V_A = -\frac{A_{12}}{6} \frac{[2a(H+a)]}{H(H+2a)} + \ln \frac{H}{H+2a} \quad (4)$$

$$V_R = \pi \varepsilon_r \varepsilon_0 a \left[(\psi_1^2 + \psi_2^2) \ln \left(\frac{\exp(2\kappa H) - 1}{\exp(2\kappa H)} \right) + 2\psi_1 \psi_2 \ln \left(\frac{\exp(\kappa H) + 1}{\exp(\kappa H) - 1} \right) \right] \quad (6)$$

where ψ is surface potential, which is replaced with zeta potential (ζ) determined from zeta potential measurement. Other parameters used such as A , a , κ , ε_r and ε_0 are adopted from the literatures, as shown in table 3.1. The radius of cells is measured from the optical images. The relationship between each interaction force (attractive force V_A and repulsive force V_R) versus separation distance (H) is carried out using MathCAD program.

Table 3.1 Parameters used in DLVO calculation

Parameter	Values
A_{ca} (Hamaker constant of CA)	6.7×10^{-21} J [40]
A_{red} (Hamaker constant of red blood cells)	9×10^{-21} J [41]
A_{leu} (Hamaker constant of leukocytes)	5×10^{-21} J [42]
a_r (Radius of red blood cell)	7×10^{-4} nm
a_n (Radius of neutrophils)	12×10^{-4} nm
a_l (Radius of lymphocytes)	10×10^{-4} nm
ε_r and ε_0	76.175 and 8.854×10^{-12} C ² /N·m ²
T (Temperature)	298 K and 310 K
κ at 298 K and κ at 310 K	4.71×10^3 and 4.618×10^3

2.3. Cell adhesion test

2.3.1. Film fabrication

a. Cellulose acetate film

CA films can be prepared using acetone as a solvent. A mixture of specified concentration of two chemicals is stirred in a closed bottle until a homogeneous solution is obtained. About 20 μ l of prepared solution is cast on a cover slip, which maintained at 40°C on a hot plate to remove the solvent by evaporation. After complete evaporation of solvent, a transparent thin film is obtained [43]. The film sample is used for further test after at least 24 hours.

b. Cellulose triacetate film

CTA film is prepared for experiment, which the method is extended from Bhat et. al. [44]. CTA polymer is dissolved in chloroform–methanol at 9:1 vol % until homogeneous solution was obtained. The film fabrication is performed followed the CA film fabrication.

The surface of CA and CTA film is observed using an optical microscope (OM) at x500 and x1000 magnification. An image processing software is used to determine roughness by calculating standard variation of gray scale images. These images for evaluation are taken at the same conditions (x500 magnification).

2.3.2. Preparation of white blood cells

Peripheral venous blood obtained from the healthy human donor is collected in tube with heparin anticoagulation. The collected blood is gently mixed by inverting test tubes six to ten times after collection. Blood sample is smeared for differential cell counting. The rest of the blood in test tube is centrifuged at 2,500 rpm 10 min at temperature of 15-20°C for separating white blood cells from red blood cells. After centrifuge, tubes are carefully removed without disturbing the red cells at the bottom. Buffy coat, which is the layer of white blood cells (WBC) cluster, is carefully collected and transferred into new tube for washing. McCoy's media with 10% plasma is added into the Buffy coat and then centrifuged at 2,500 rpm for 10 minutes at 15°C. Finally, media is leave and then the number of white blood cells is counted with hemocytometer before using in experiment.

2.3.3. Cell adhesion test

One milliliters of media which contained about $2-4 \times 10^6$ cells/ ml is added on CA and CTA films. The films are incubated at 37°C with humidity of 5% CO_2 for 1, 2, and 3 hours. After that, samples are washed for 3-4 times with 1x PBS (pH 7.4) until debris particle completely removed. Cells on film samples are fixed with 0.1% glutaraldehyde for 1 min to preserve the structure of cells then wash off with distilled water and dye strained with dip quick method. This dye is composed of methylene blue and safanine. The stained membranes are rinsed with water and then placed on glass slide to dry at room temperature. The cells adhesion appearances on samples are observed by OM.

CHAPTER IV

RESULTS

1. Zeta Potential Measurement

Surface charge of cellulose acetate (CA) and cellulose triacetate (CTA) polymer is determined in polyvinylpyrrolidone (PVP) solution with pH of 7.4 and viscosity of 30 mPa·s and compared with surface charge of blood cells composing of red blood cells (RBC), neutrophils and lymphocytes. The zeta potential of each particle is determined at different temperature i.e. 298K and 310K and results are reported in figure 4.1 and figure 4.2.

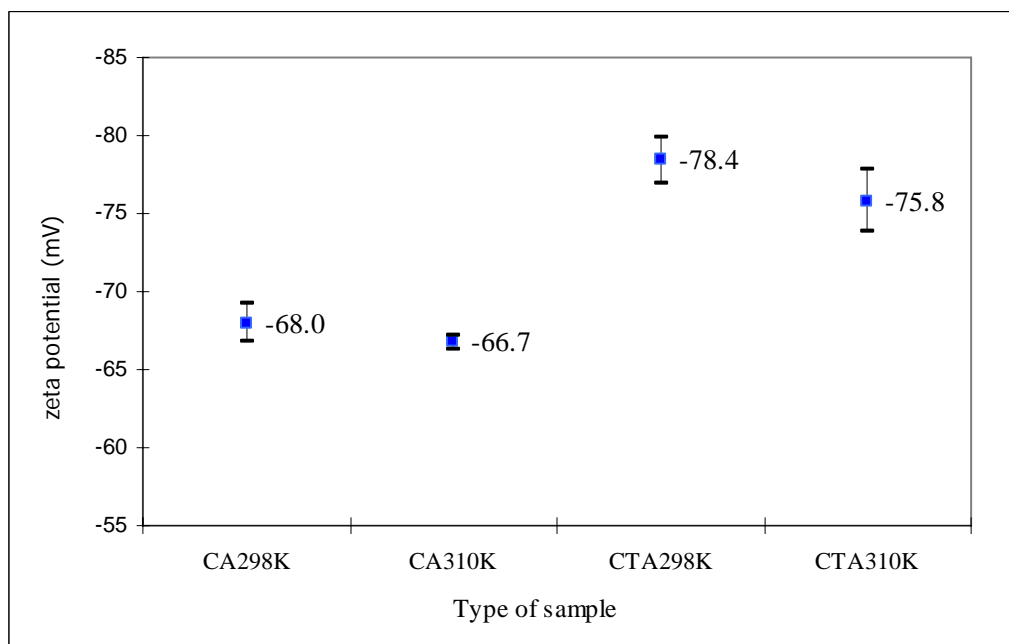


Figure 4.1 Zeta potential of CA and CTA polymer in 5% PVP with pH 7.4 at 298 K and 310 K (Bar = SD)

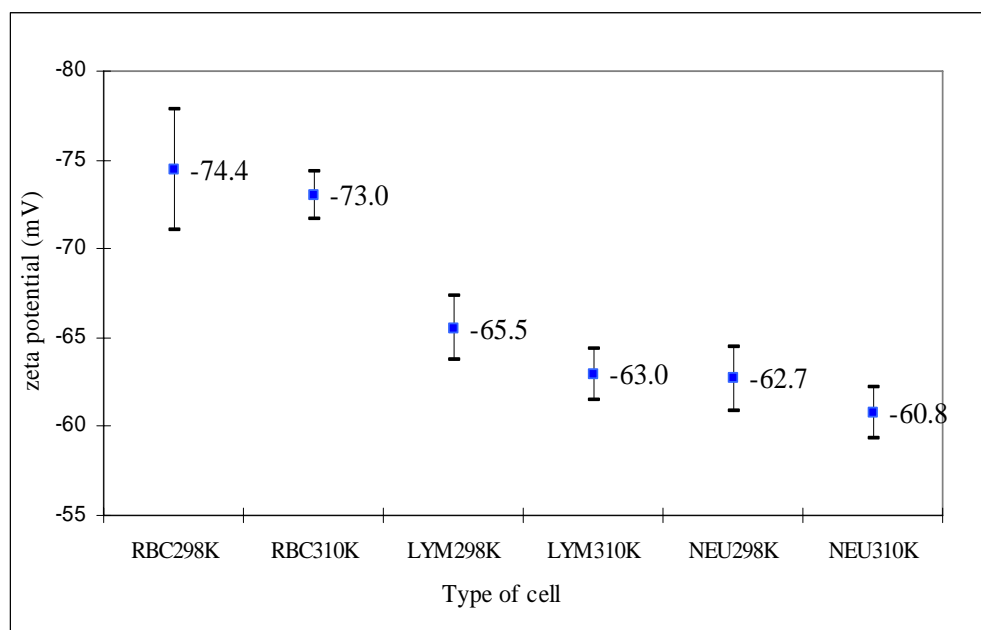


Figure 4.2 Zeta potential of RBC, neutrophils and lymphocytes in 5% PVP with pH 7.4 at 298 K and 310 K (Bar = SD)

2. Interaction Force Calculation

The interaction force between each blood cells type on each substrate compose of repulsive force (V_R) and attractive force (V_A), which are calculated from DLVO equations i.e. equation (4) and equation (6). The net interaction force is calculated from summation of repulsive force and attractive force, which represents minimum separation distance of cells before adhesion.

2.1. Attractive force

The attractive force calculates from equation (4), which each parameter reviewed from literatures as shown in table 3.1. Results of attractive force between each cell type and cellulose substrate is shown in figure 4.3. The attractive force of each type of blood cell on CTA substrate and CA substrate are the same due to the same Hamaker constant used.

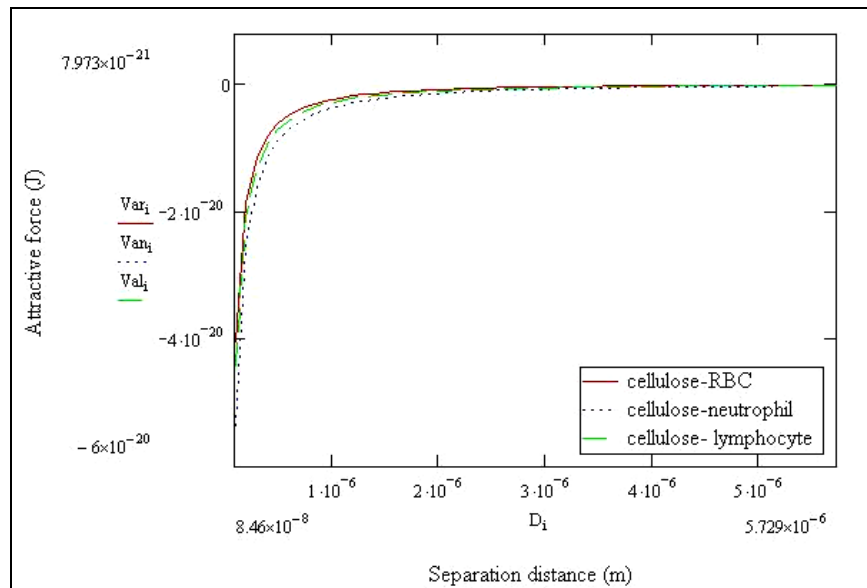


Figure 4.3 The attractive force between cellulose substrate and human blood cells composed of RBC, neutrophils and lymphocytes

2.2. Repulsive force

Repulsive force between each substrate and each blood cell type is calculated from equation 6 as shown in figure 4.4 to figure 4.7, which zeta potential is determined in different temperature i.e. 298 K and 310 K.

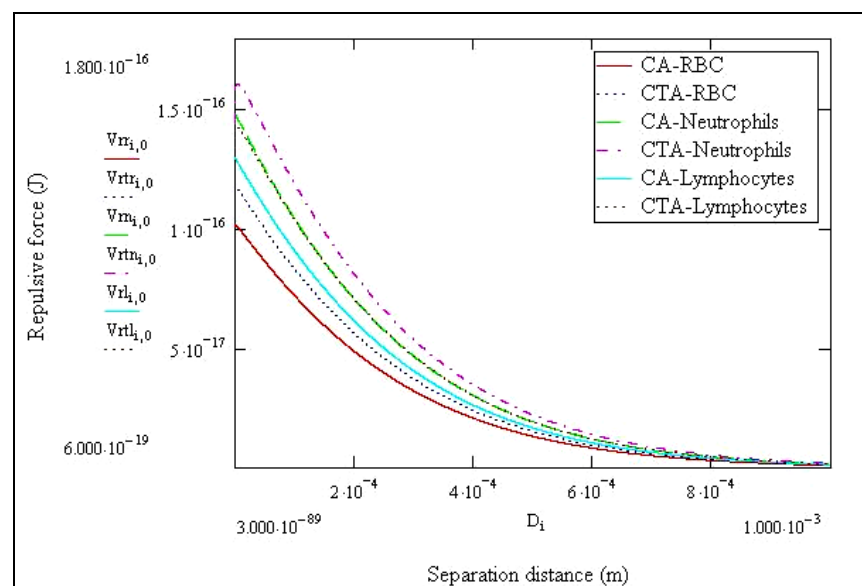


Figure 4.4 The repulsive force between each cells type and both substrates at 298 K

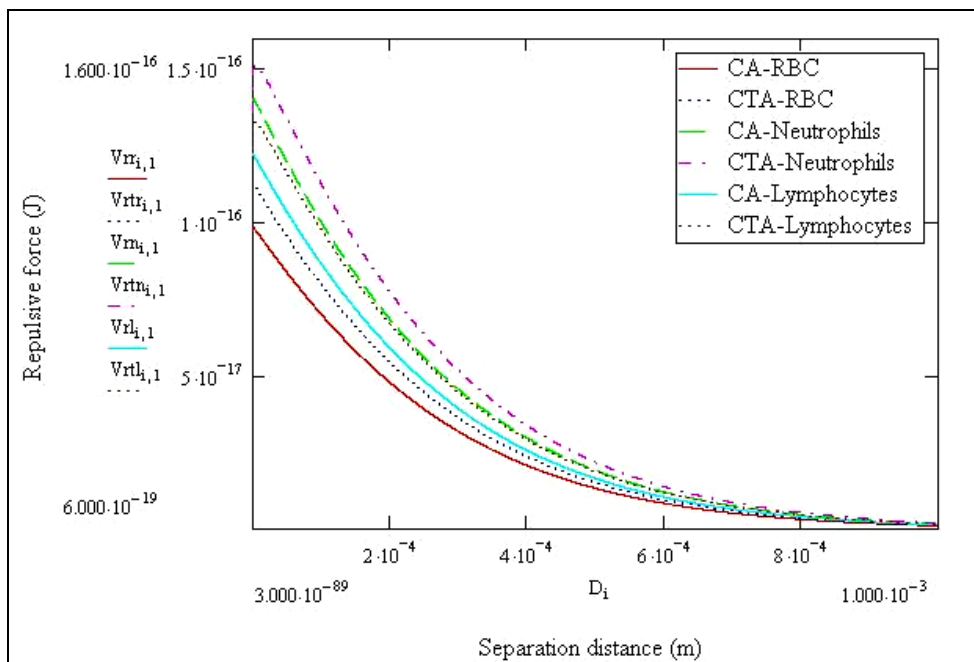


Figure 4.5 The repulsive force between each cells type and both substrates at 310 K

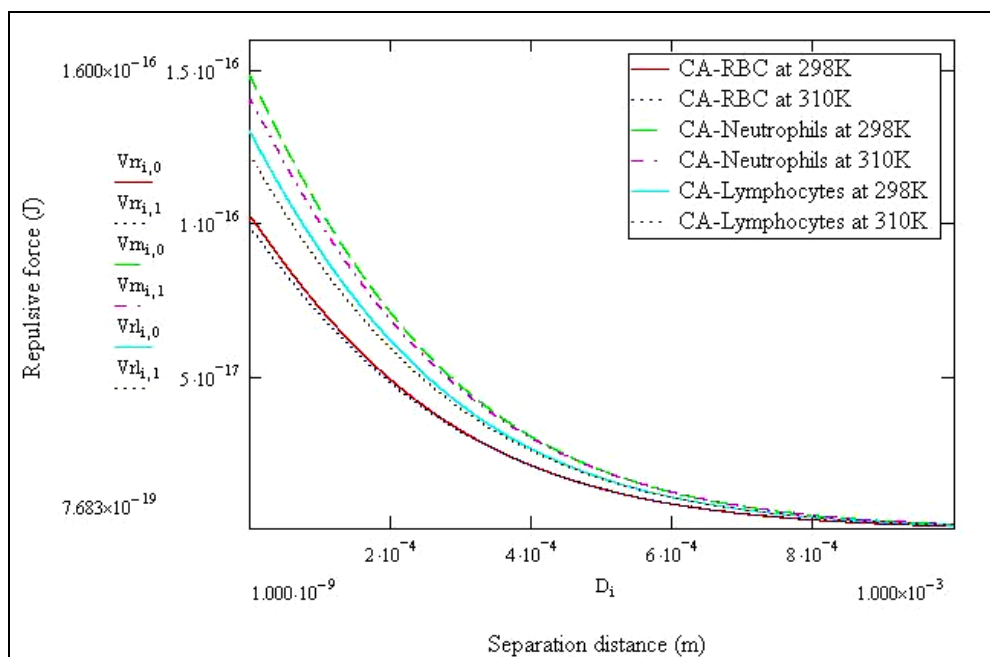


Figure 4.6 The repulsive force between each cells type and CA substrate at 298 K and 310 K

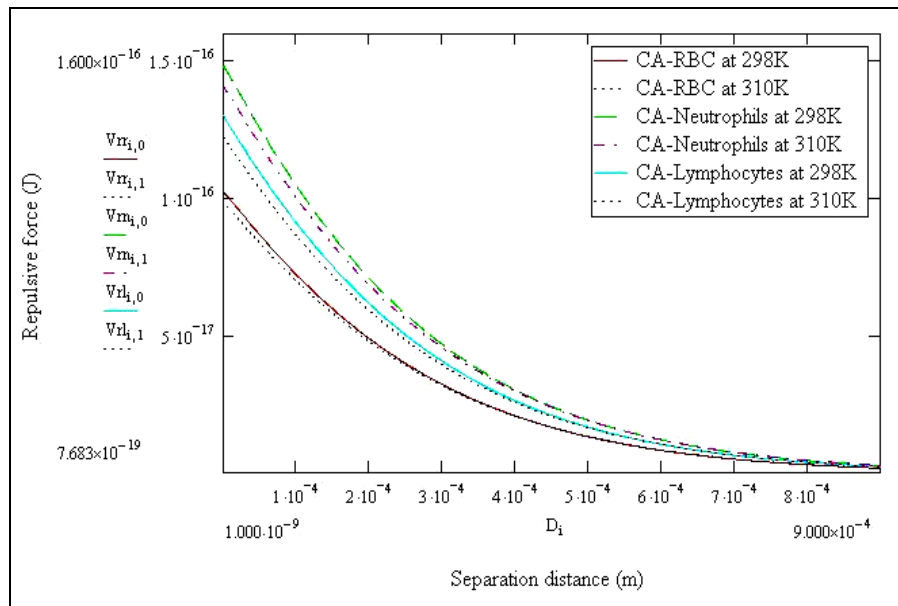


Figure 4.7 The repulsive force between each cells type and CTA substrate at 298 K and 310 K

2.3. Net interaction force

The net interaction force between each substrates and each blood cell type is shown in figure 4.8 to figure 4.11.

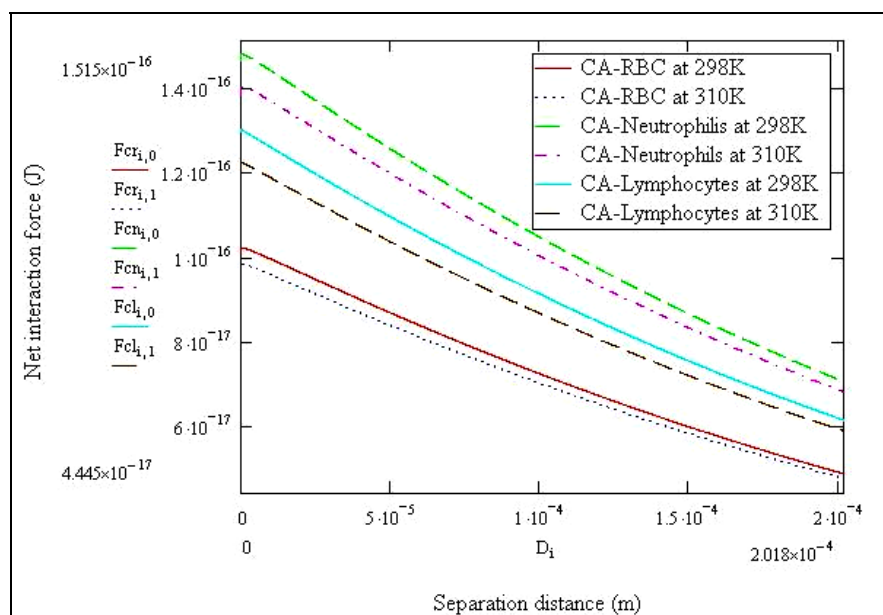


Figure 4.8 The net interaction force between CA and each blood cell type at different temperatures

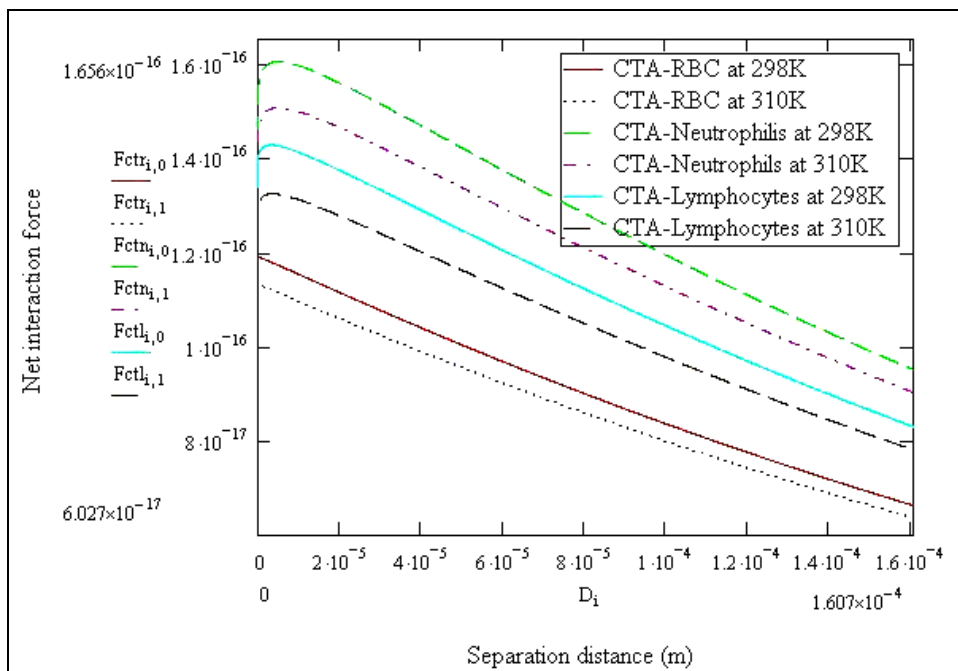


Figure 4.9 The net interaction force between CTA and each blood cell type at different temperatures

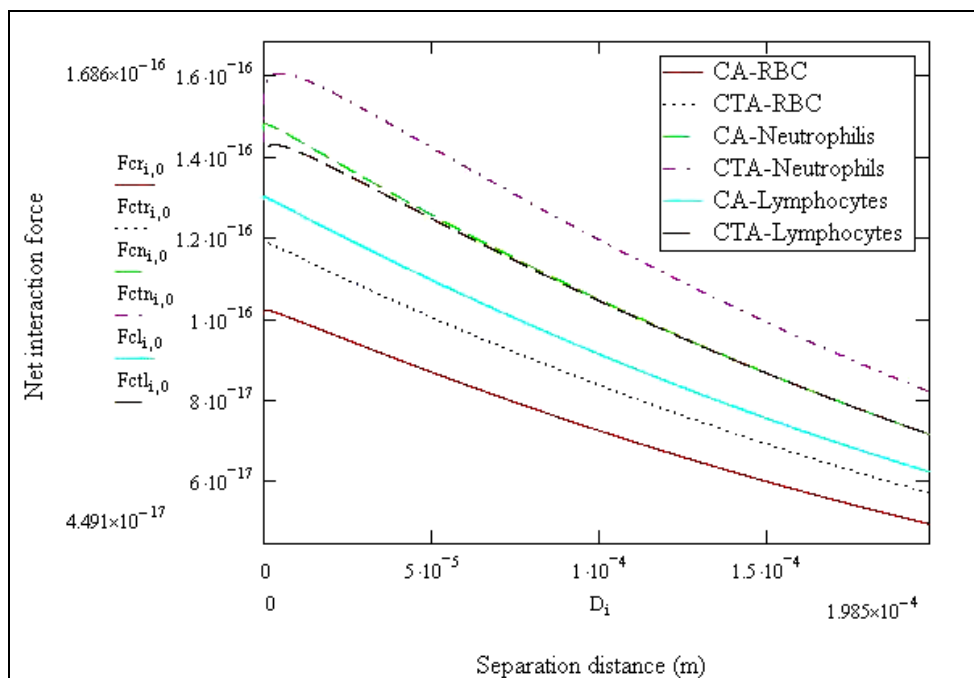


Figure 4.10 The net interaction force between each substrate and each blood cell type at 298 K

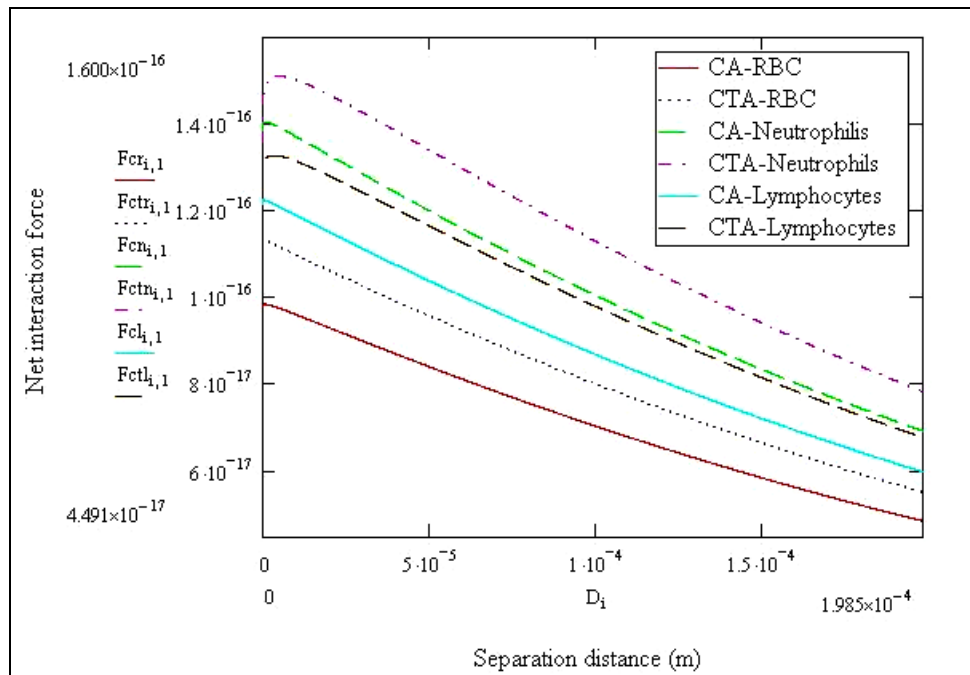


Figure 4.11 The net interaction force between each substrate and each blood cell type at 310 K

3. Cell Adhesion Test

3.1. Surface morphology of films

CA and CTA film is fabricated at different polymer contents (5g/100ml and 10g/100ml). The surface morphology of CA and CTA films is observed before cells cultivation. For the same polymer type, there is slightly different roughness between both polymer contents as show in figure 4.12 and figure 4.13.

These films are dense in structure by water absorption testing which no permeation are observed on both CA and CTA film. These films are then used for cell adhesion testing where the interaction force between various blood cells on these substrates is estimate by the aid of DLVO theory.

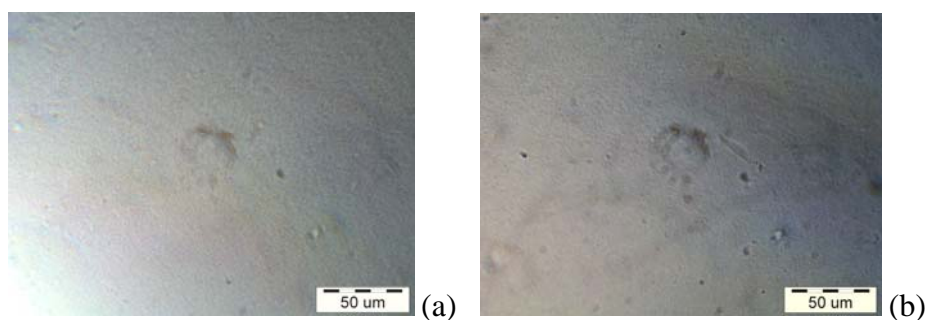


Figure 4.12 Surface morphology of CA films from OM at x500 magnification;
(a) CA5 (b) CA10

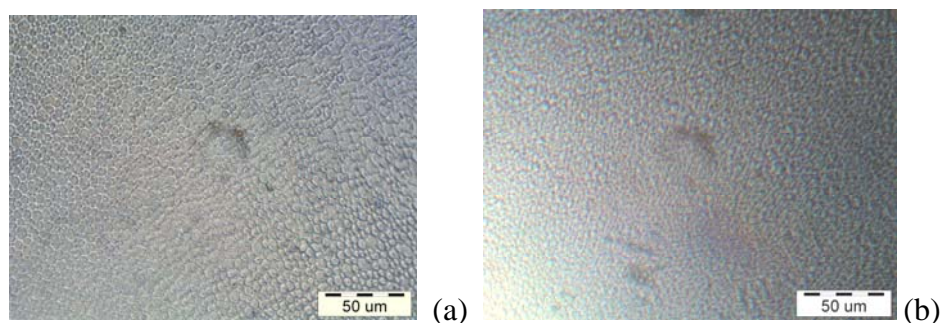


Figure 4.13 Surface morphology of CTA films from OM at x500 magnification;
(a) CTA5 (b) CTA10

In order to determine the surface roughness of the samples, the variation of image intensity in each sample obtained from the optical microscope are analyzed using image processing software (Image J) as shown in table 4.1.

Table 4.1 The SD value of roughness calculated from Image J program

Substrates	SD ($\bar{x} \pm SD$)
CA5	10.12 \pm 0.19
CA10	8.47 \pm 0.49
CTA5	19.43 \pm 0.45
CTA10	17.56 \pm 1.16

3.2. Cell adhesion appearances

About 1 ml with $2.5 (\pm 0.3) \times 10^6$ of white blood cells suspensions is prepared for cell adhesion test and table 4.2 shows the original number of each cell type counted

by differential cell count method. After incubation time, the number of cells adhered on each substrate is observed referring to original number by OM and reported in cells number per mm² as shown in figure 4.14. Also, the type of blood cells adhered on surface is counted and reported.

Table 4.2 The number of cell differential count from blood with heparin anticoagulant (n=3)

	Neutrophil	Lymphocyte	Monocyte	Basophil	Eosinophil
% of cells ($\bar{x} \pm SD$)	44 ± 1.5	53 ± 1.5	2 ± 0.6	1 ± 0.6	1 ± 0.6

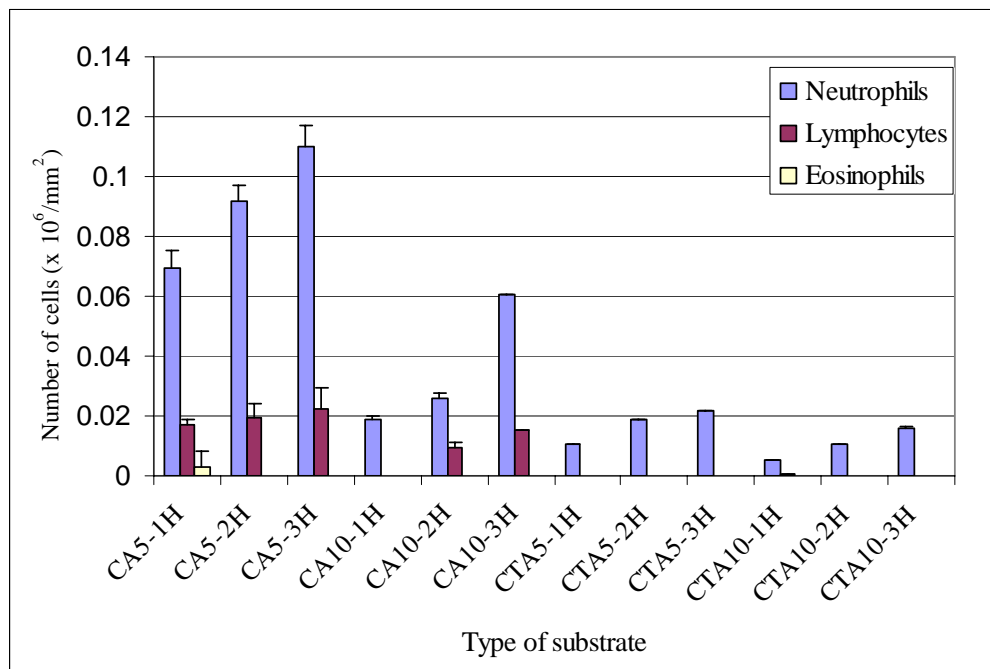
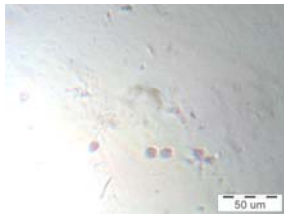
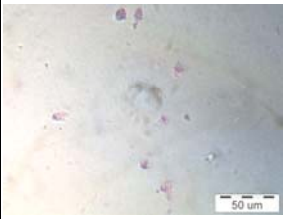
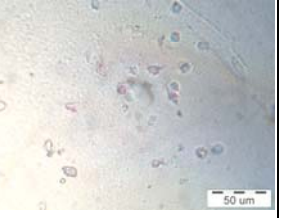
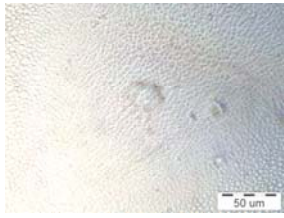
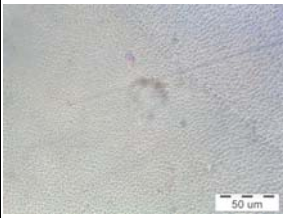
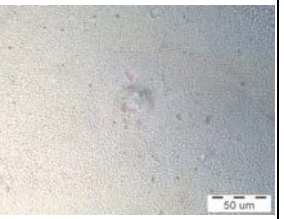


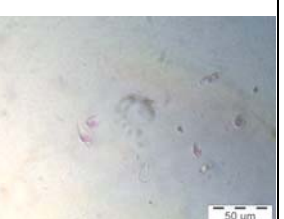





Figure 4.14 The mean number of neutrophils, lymphocytes and eosinophils (x10⁶ cells/ mm²) adhered on different substrates at 1, 2 and 3 hours incubation (Bar = SD, n=3)

During process, the optical images of cell on each substrate at x1000 magnification are shown in table 4.3.

Table 4.3 Blood cells adhered on different substrate for incubation period of 1, 2 and 3 hours from OM at x500 magnification

Sample ID	Time of incubation (hour)		
	1	2	3
CA5			
CTA5			
CA10			
CTA10			

CHAPTER V

DISCUSSION

The results of each experiment are discussed and evaluated based on DLVO theory as follows.

1. Zeta potential measurement and interaction force estimation

According to the zeta potential (ζ) measurements, the zeta potential of cellulose polymer both cellulose triacetate (CTA) and cellulose acetate (CA) are negatives (see figure 11-12). The amplitude of the zeta potential on CTA is larger than that of CA substrate due to the functional group presenting in CA and CTA. The substitution of $-\text{COOCH}_3$ in cellulose structure leading to the different zeta potentials measured as well as the high density of $-\text{COOCH}_3$ also leading to a higher negatively charge presenting on CTA. Moreover, this substitution of $-\text{COOCH}_3$ on $-\text{OH}$ functional group reduces the hydrophilicity of the cellulose substrate as the lost of $-\text{OH}$ functional group.

The zeta potentials of various cells were also determined including red blood cells (RBC), neutrophils, and lymphocytes. The results showed that the RBC possesses the strongest negative surface charge than that of the others. Therefore the stability of zeta potential of each blood cell are $\text{RBC} > \text{lymphocytes} > \text{neutrophils}$. This may due to the complexity of the blood cell structure especially the protein type on surface. Generally, blood cells membrane, plasma membrane, is consisted of lipid and protein. The different in protein/lipid ratio [45] contribute to the difference in surface charge.

General, blood cells membrane or call plasma membrane is consisted of lipid and protein components, which the protein/ lipid ratios of each cell type are different [45] and this should be a factor that led to different charge on surface. The evaluation of zeta potential of each sample was performed at 298 K and 310 K. It is found that by increasing the temperatures, the amplitude of zeta potential is slightly decreased. This

may due to the change of the temperature that affected on the viscosity of the media (PVP) which agree well with a study by [46], whose results showed that the viscosity of PVP is slightly increased when temperature decreased. Moreover, Cinar [17] represented the relationship between temperature and viscosity of blood using capillary tube viscometer. They showed that when temperature decreased from 36.5°C to 22°C, blood viscosity increased 26.13% while blood flow rate decreased. The increasing of blood viscosity altered the velocity of colloid particles during zeta potential measurement.

The interaction force calculations from attractive and repulsive forces were performed based on DLVO theory. The Hamaker constants and zeta potential measurement of each material were use for modeling. However, the determination of Hamaker constants is very difficult. Therefore, the Hamaker constant of white blood cell, red blood cell, and cellulose substrate were adopted from Sun et. al. [42], Parsegian et. al. [41] and Winter et. al. [40], respectively. The results of attractive force (V_A) between blood cells and substrate surface were depicted in figure 13 as a function of the distant between them. This showed that when cell approaching toward the substrate surface, the attractive force tend to be decreased. The effect of cell types on attractive force estimation on cellulose substrate showed that the red blood cell has the weakest attraction compare to the white blood cells at the same distance away from the substrate surface. However, the white blood cells (neutrophil and lymphocyte) which possess the same Hamaker constant yield a different in the attraction force calculation as seen in figure 13. This larger white blood cell, neutrophil (12 μ m), yields a larger attractive force comparing to a smaller white blood cell, lymphocytes (10 μ m). These results indicate that the geometry of the surfaces has a large effect on the attraction force between two surfaces.

The repulsive force estimation using measured zeta potential showed that the CTA surface has a stronger repulsion force comparing to that of CA substrate (see figure 14 and figure 15), due to a larger zeta potential of CTA (-78.4 mV at 298K and -75.8 mV at 310K) (see figure 11). Indicating that the CTA has a stronger repulsion than that of CA substrate, therefore, hydrophobic blood cells tend to be attached on CA substrate. Moreover, the repulsion force estimation of various cell types at different temperatures (298K and 310K) showed that by increasing the temperature the

repulsive force on each cell types on both CA and CTA are decreased due to the weakness of the surface charge on the cells from zeta measurement and the reduction of PVP viscosity at a higher temperature (~ 30 cP) (see figure 16 and 17).

By combining the attraction and repulsion forces together, the net interaction force of each blood cell on both CA and CTA substrates were obtained meaning the energy barrier appearing between cells and each polymer substrates. The results of net interaction forces of various blood cells on CA substrate at 298K and 310K were shown in figure 18. These showed that the neutrophils on CA substrate has the strongest energy barrier of 1.404×10^{-16} J at 310 K followed by lymphocytes (1.224×10^{-16} J) and RBC (9.84×10^{-17} J) respectively (see figure 18). By increasing the temperature, the energy barrier of each cell interaction decreased due to the reduction of zeta potential as well as the viscosity of PVP media. This reduction of viscosity causing the colloid cells to be move easier than that in a viscose fluid. The similar trends also observed on CTA substrates with various cell types (see figure 19).

2. Cell adhesion test

CA and CTA films were prepared at different composition i.e. 0.05 g/ml (CA5 and CTA5) and 0.1 g/ml (CA10 and CTA10) following Bhat et. al. [44]. The surface morphology of the film samples were evaluated using an optical microscope (OM) at x500 magnification as shown in figure 22 and 23. Then, films were incubated with white blood cells suspensions at 310 K for 1, 2, and 3 hours, the samples were then rinsed with PBS and the attached celled were evaluated using an optical microscope (OM) at x1000 magnification.

On the study of the cellulose concentration effect on the substrates, the roughness estimation using image processing software (Image J) showed that the CA and CTA films prepared using a higher polymer content (CA10 and CTA10) have a higher roughness when comparing with those prepared at a lower content (CA5 and CTA5) (see table 4.1), which corresponding to the images from OM. This surface roughness may due to the evaporation rate of solvent during the film casting step. During the preparation of these polymer solutions, a lower polymer content cellulose substrate has a faster evaporation comparing to the higher polymer content solution due to a larger solvent content in the precursor. Thus, the surface cellulose film having

a higher solvent content may become rougher. By comparing between the substrate constructed at different polymer contents, the higher content substrates (both CA and CTA) have a lower number of blood cells on the surface. This may be due to the difference in roughness of the substrate surface that mentioned earlier.

Although, the roughness may contribute to the difference in cell adhesion on substrate, the roughness of substrates prepared from CTA polymer is slightly more than that from CA polymer as shown in figure 4.12 and 4.13. The roughness estimation using Image J also showed that CA surface is smoother than CTA surface (see table 4.1). This may be due to the type and properties of solvent applied in this study. By dissolving polymers in a similar hydrophilic solvent, such as CA in acetone, a homogeneous solution of CA is obtained while the solution of CTA in these solvent may not form a homogeneous solution since CTA is more hydrophobic than CA. This formation of hydrogen-bonding phenomenon of water or other hydrophilic agent on CA polymer was investigated by van Oss et. al. [47] and Hai-Qing et. al. [48]. The hydrophilic solvent induces the hydrophilic surface of the polymer film by rearranging the hydrophilic tail of the polymer in outward direction during evaporation period. Thus the surface of the polymer film becomes hydrophilic. On the other hand if hydrophobic solvent is used the surface of cast polymer becomes hydrophobic due to the rearrange of hydrophobic tail of the polymer in the direction that solvent evaporating. Therefore, the type and properties of solvent used should be considered because it effects the rearrangement of the polymer molecule during film preparation and also led to the different surface morphology of the samples.

When the cell adhesions on both substrates were observed, the results showed that the CTA films contain less number of blood cells especially white blood cells than that of CA films (see figure 4.14). This may be due to the hydrophilic/ hydrophobic properties of polymer, which related to the percent of functional group presenting in the film samples. The Federal Trade commission defined that there are about 92% of hydroxyl group (-OH) in CTA were substituted with other functional groups leading to the decreasing of hydrophilic property of CTA polymer compared to the CA. On the other hands, a higher percentage of -OH group on CA causes a larger degree of hydrophilicity in these samples. Thus the adhesion of blood cells is usually found on

CA surfaces. Moreover, the presence of –OH group also increases the effectiveness of water adsorption therefore the cells tend to be attached on CA surface.

Furthermore, the relationship between surface charge and cells adhesion appearances found that CTA substrate, which has a stronger negative charge than that of CA substrate, provide a smaller numbers of cell adhesion on surface comparing to that on CA surface. Warner et. al. [30] and Voravee et. al. [26] suggested that functional group on material surface can influence on zeta potential measurement. Therefore, the different degree of –OH substitution between CA and CTA may be the reason of the difference in zeta potential measured and the different in appearance of cell numbers on surface. Thus, the zeta potential measured is related to the hydrophilic/ hydrophobic properties of the materials.

Most of the cells found on all substrates are neutrophils (see figure 4.14). This may be due to the scavenging functions of neutrophils when encounter the foreign body in an inflammation process. Generally, neutrophils can be activated by solid surface resulting in adherence similar to that of monocytes/ macrophages. Moreover, the longer the incubation period, the large number of cells attached to the substrate.

On the other hand, RBC showed the lowest energy barrier, however, we rarely observed RBC on both substrates. This may be due to the fact that RBC is deformable. This property prevents RBC from adherence to any surface. Another reason is that RBC do not contain nucleus therefore the activation from solid surface is not possible to induce adherence.

3. The relationship between the net interaction forces based on DLVO theory and blood cell adhesions

The interaction forces between various blood cells; RBC, neutrophils, and lymphocytes on cellulose substrate are estimated. These interaction forces are then compared to blood cells adhesion observed in experiment. By comparing the net interaction force on various blood cells on CA and CTA in figure 22 and 23 respectively with the cells adhesion observed using an optical microscope in figure 27, the interaction force between neutrophils on both substrates yield the highest energy barrier compared to the other cells, which is opposite to the results observed from the OM. This may be due to the following reasons:

1. Protein production by neutrophils

Blood cells especially neutrophils may be activated when exposed to an artificial substance. This causes neutrophils to express various proteins such as a group of adhesion protein on the cell surface. These proteins could alter the surface charge of the cells, therefore interfere the interaction force estimated by DLVO theory.

2. The different constituent in medium

The zeta measurement for repulsion force evaluation was performed in PVP solution to mimic the viscosity of the blood. This high viscosity of PVP prevents the precipitation of blood cell during the zeta measurement. However, by using PVP as the medium, the content of PVP is different from that of blood. This could cause the different outcome in cell adhesion by estimation of DLVO theory.

3. The surface roughness

Suresh et. al. [49] showed the significance of the surface roughness on the attractive force using DLVO theory. This model is the interaction force between rough sphere polystyrene latex having various asperities on the smooth surface glass substrate. The radius of asperity (ϵ_s) is incorporated in DLVO theory, the result of the total interaction forces are shown that the energy barrier of the interaction force decreases from 2990 kT/mm for perfectly smooth surfaces to about 50 kT/mm when 20 nm asperities are presented. Their study demonstrated that the roughness of cells surface may influence on the net interaction by increasing the vdW attraction. This reason corresponds with the cell adhesion results in this experiment. The number of neutrophils appearance was high because of the roughness of their surface (as shown in figure 26). Therefore, the roughness of the surface should be incorporated into the DLVO theory for the net interaction force calculated between cells and CA or CTA substrates.

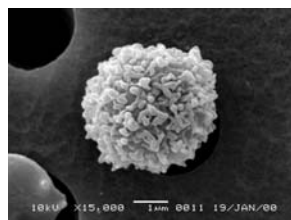


Figure 5.1 White blood cell morphology at x15,000 magnification via SEM (Photo from <http://embryology.med.unsw.edu.au/Notes/heart20.htm> [50])

4. Blood cells geometry

Cell geometry affects the interaction force from DLVO theory. The estimation of interaction force between blood cells and cellulose substrates was based on the assumption that all blood cells are spheres in shape and the substrates were smooth flat surfaces. However, this assumption may not be suitable for all types of cells, especially for the red blood cell which has a biconcave disc structure. The shape factor should be integrated in the estimation of interaction force. Moreover, to illustrate the effect of the cell size on the interaction force estimation, the size of each cell was manipulated to be the same (6 μm) and the interaction force was evaluated. These results showed that the RBC on CA substrate has the strongest energy barrier of 1.687×10^{-16} J, followed by lymphocytes (1.469×10^{-16} J) and neutrophils (1.404×10^{-16} J) respectively, which correspond to the results observed from the OM (see figure 4.14) and correspond to the amplitude of zeta potential measurement (see figure 4.2). This assumption represents that the size of cells strongly influenced the evaluation of interaction force calculated from DLVO theory.

5. Hamaker constant of various blood cells

The Hamaker constant of white blood cells used in this study was adopted from previous reports. Therefore, the results of net interaction force may not be reliable. The Hamaker constants of biological matters are difficult to measure due to the complicated techniques of Atomic Force Microscopy (AFM). The interesting cells must be attached onto the tip of the cantilever and placed on the substrate. The lifting force required to detach cells from the substrate is used in the evaluation of the Hamaker constant for each cell type.

CHAPTER VI

CONCLUSION

The zeta measurement of various blood cells and cellulose substrates showed that the all zeta potential of the cells and cellulose substrates are negatives. The amplitude of the surface charge of various blood cells are RBC > lymphocytes > neutrophils, as well as the amplitude of zeta potential on cellulose substrates are CTA > CA. These indicate that the electrostatic repulsions of blood cells on CTA are greater than that of CA which could be observed in the cell adhesion testing experiments. Moreover, the strong surface charges of RBC from zeta measurement contribute to the strong repulsion of the RBC on cellulose substrate. However, the interaction force based on DLVO theory showed that the energy barriers of neutrophils > lymphocyte > RBC which contrast to the cell adhesion experiments. This may due to the following reasons;

1. Protein formation by neutrophils in PVP media
2. The different constituent of protein and electrolyte in media
3. The surface roughness of the cells and substrates
4. Blood cell geometries
5. Hamaker constant of various blood cell

Therefore, it may be concluded that the interaction force estimation of various blood cells on cellulose based substrates depending on various factors i.e. the Hamaker constants, the surface geometry, surface roughness, hydrophilicity, surface charge, of both cells and substrate. The complication of the interaction between cell and substrate may influenced by the cell activity in the media or substrates. Therefore, these factors may be further investigated to delineate the understanding to blood cell adhesion phenomena on various substrates in the future.

REFERENCES

1. Williams DF. The Williams dictionary of Biomaterials. 1999.
2. William L. Henrich. Principles and practice of dialysis. 3rd ed. USA: Lippincott Williams & Wilkins; 2004.
3. Charles Frederick Cross. [cited 2006 6 June]; Available from: <http://www.answers.com/topic/charles-frederick-cross>
4. Richard WB. Membrane technology and applications. New York: McGraw-Hill; 2000.
5. Wytze PO, Menno de M, Adrian W, Mohammed RD, Roy HG. In Vivo Evaluation of Four Hemodialysis Membranes: Biocompatibility and Clearances. *Dialysis & Transplantation*. 1995 August;24(8):450-458.
6. Hoenich NA, Stamp S. Clinical investigation of the role of membrane structure on blood contact and solute transport characteristics of a cellulose membrane. *Biomaterials*. 2000;21:317-324.
7. Hiraishi K, Takeda Y, Shiobara N, Shibusawa H, Jimma F, Kashiwagi N, Saniabadi AR, Adachi M. Studies on the Mechanisms of Leukocyte Adhesion to Cellulose Acetate Beads: An In Vitro Model to Assess the Efficacy of Cellulose Acetate Carrier-based Granulocyte and Monocyte Adsorptive Apheresis. *Therapeutic Apheresis and Dialysis*. 2003;7(3):334-340.
8. Deppisch R, Storr M, Buck R, Gohl H. Blood material interactions at the surfaces of membranes in medical applications. *Sep Purif Technol*. 1998;14:241-254.
9. Hoenich NA, Stamp S, Roberts SJ. A microdomain-structured synthetic high-flux hollow-fiber membrane for renal replacement therapy. *ASAIO J*. 2000;46:70-75.
10. Kataoka K. High-capacity cell separation by affinity selection on synthetic solid-phase matrices. In: Dhinakar S, Kompala, Paul Todd, editors. *Cell separation science and technology*. Washington, DC American Chemical Society; 1991. p. 159-174.

11. Kataoka K, Sakurai Y, Tsuruta T. *Makromol Chem Suppl.* 1985;9:53.
12. Maggiore Q, Enia G, Catalano C, Misefari V, Mundo A. Effect of blood cooling on cuprophan-induced anaphylatoxin generation. *Kidney Int.* 1987 Dec;32(6):908-911.
13. William R, Dayong G. Properties of membranes used for hemodialysis therapy. *Seminars In Dialysis.* 2002 January-February;15(1):191-195.
14. Cellulose triacetate. [cited 6 June 2006]; Available from: <http://en.wikipedia.org/wiki/Triacetate>
15. Pichaiwong W, Leelahavanichkul A, Eiam-ong S. Efficacy of cellulose triacetate dialyzer and polysulfone synthetic hemofilter for continuous venovenous hemofiltration in acute renal failure. *J Med Assoc Thai.* 2006 Aug;89 Suppl 2:S65-72.
16. Frederic HM, Edwin FB. *Essentials of anatomy&physiology.* New Jersey, USA: Prentice Hall, Inc.; 1997.
17. Cinar Y, Senyol AM, Duman K. Blood viscosity and blood pressure: role of temperature and hyperglycemia. *American Journal of Hypertension.* 2001;14(5):433-438.
18. Buddy DR, Allan SH, Frederick JS, Jack EL. *Biomaterials science: An introduction to materials in medicine.* California, USA: Academic Press; 1996.
19. Buddy D. Ratner, Allan S. Hoffman, Frederick J. Schoen, Lemons JE. *Biomaterials science: An introduction to materials in medicine.* California, USA: Academic Press; 1996.
20. Stuart L Cooper, Nicholas A Peppas. *Biomaterials: Interfacial phenomena and applications.* USA: American Chemical Society; 1982.
21. Hanson SR. Blood-Material Interactions. In: Gary E. Wnek, Bowlin GL, editors. *Encyclopedia of Biomaterials and biomedical engineering.* New York: Marcel Dekker, Inc. p. 1-882.
22. Falkenhagen D, Brown GS, Thomaneck U, Levin NW, Ivanovich P, Bergstrom J, Kishimoto T, Klinkmann H. Behaviour of white blood cells and the complement system. *Nephrol Dial Transplant.* 1993;8(2):8-14.

23. Grooteman MP, Nube MJ, van Limbeek J, Schoorl M, van Houte AJ. Lymphocyte subsets in dialyser eluates: a new parameter of bioincompatibility? *Nephrol Dial Transplant*. 1996 Jun;11(6):1073-1078.
24. Arthur W. Adamson, Alice P. Gast. *Physical chemistry of surfaces*. USA: John Wiley & Sons, Inc.; 1997.
25. Factors that influence the adhesion - Wetting of the surface. In: wetting.gif, editor. www.google.com: SpecialChem S. A.; 2007.
26. Voravee P Hoven, Varawut Tangpasuthadol, Yaowamand Angkitpaiboon, Kiatkamjornwong S. Selective protein adsorption of surface-charged chitosan. 31st Congress on Science and Technology of Thailand; 2005 18 – 20 October 2005; Suranaree University of Technology; 2005.
27. Lyklema J. *Fundamentals of interface and colloid science*. London: Academic Press; 1991.
28. Arthur WA, Alice PG. *Physical chemistry of surfaces*. USA: John Wiley & Sons, Inc.; 1997.
29. Dixon T. Electroosmotic flow In: stern_layer.jpg, editor. www.google.com.
30. Werner C, König U, Augsburg A, Arnhold C, Korber H, Zimmermann R, Jacobasch HJ. Electrokinetic surface characterization of biomedical polymers - a survey. *Colloids and Surfaces A: Physicochemical and Engineering Aspects*. 1999;159:519-529.
31. DeJaguin BV, Kolloid BV. On the repulsive forces between charged colloid particles and on the theory of slow coagulation and stability of lyophobic sols. *Trans Faraday Soc*. 1940;35:203 - 215.
32. Hermansson M. The DLVO theory in microbial adhesion. *Colloids and Surfaces B: Biointerfaces*. 1999;14(1-4):105-119.
33. Zeta-Meter I. *Zeta Potential: A Complete Course in 5 Minutes*.
34. Bergström L, Stemme S, Dahlfors T, Arwin H, Ödberg L. Spectroscopic Ellipsometry Characterisation and Estimation of the Hamaker Constant of Cellulose. *Cellulose*. 1999;6:1-13.
35. Lyklema J. *Fundamentals of interface and colloid science*. London: Academic Press; 1991.

36. Verwey EJW, Overbeek JThG. Theory of the Stability of Lyophobic Colloids. first ed. New York: Elsevier Publishing Company Inc; 1948.
37. Hogg RI, Healy TW, Fuerstenau DW. Mutual coagulation of colloidal dispersions. *Trans Faraday Soc.* 1966;62:1638 - 1651.
38. Hayashi H, Tsuneda S, Hirata A, Sasaki H. Soft particle analysis of bacterial cells and its interpretation of cell adhesion behaviors in terms of DLVO theory. *Colloids and Surfaces B: Biointerfaces.* 2001;22(2):149-157.
39. Adamczyk Z, Weron P. Application of the DLVO theory for particle deposition problems. *Advances in Colloid and Interface Science.* 1999;83:137-226.
40. Winter L. Lic. Thesis. Stockholm: Dept. Paper Technology; 1987.
41. Parsegian VA, Gingell D. Red blood cell adhesion. III. Analysis of forces. *J Cell Sci.* 1980 February 1, 1980;41(1):151-157.
42. Sun C, Migliorini C, Munn LL. Red Blood Cells Initiate Leukocyte Rolling in Postcapillary Expansions: A Lattice Boltzmann Analysis. *Biophys J.* 2003 July 1, 2003;85(1):208-222.
43. Cenci A, Koren S, Filipi B, Stropnik C. Porcine blood cell separation by porous cellulose acetate membranes. *Cytotechnology.* 1998;26:165-171.
44. Bhat NV, Wavhal DS. Preparation of cellulose triacetate pervaporation membrane by ammonia plasma treatment. *Journal of Applied Polymer Science.* 2000;76(2):258-265.
45. Popov S, Ovodova R, Popova G, Nikitina I, Ovodov Y. Adhesion of human neutrophils to fibronectin is inhibited by comarum, pectin of marsh cinquefoil *Comarum palustre* L., and by its fragments. *Biochemistry (Moscow).* 2005;70:108-112.
46. McDonald HJ, Spitzer RH. Polyvinylpyrrolidone: The Electromigration Characteristics of the Blood Plasma Expander. *Circ Res.* 1953 September 1, 1953;1(5):396-404.
47. van Oss CJ. Interfacial forces in aqueous media. New York, USA: Marcel Dekker, Inc.; 1994.
48. Hai-Qing Liu L-NZATTM. Water solubility of regioselectively 2,3-O-substituted carboxymethylcellulose. *Macromolecular Rapid Communications.* 1997;18(10):921-925.

49. Suresh L, Walz JY. Effect of Surface Roughness on the Interaction Energy between a Colloidal Sphere and a Flat Plate. *Journal of Colloid and Interface Science*. 1996;183:199-213.
50. Mark H. Cardiovascular System - Blood. In: <http://embryology.med.unsw.edu.au/Notes/images/rbcm.jpg>, editor. www.google.com; 2007.

APPENDIX

APPENDIX A

INTERACTION FORCE ESTIMATION BY DLVO THEORY OF VARIOUS BLOOD CELL TYPES ON CELLULOSE SUBSTRATES

Interaction force between different types of blood cell on CA and CTA

$$i := 1 \dots 10000 \quad D_i := \frac{i}{100000000}$$

$$j := 0 \dots 1$$

$$T_w := (298 \text{ } 310) \quad k := 1.38 \cdot 10^{-23} \text{ at pH is } 7.4 \quad \epsilon_p := 76.175 \quad \epsilon_0 := 8.854 \cdot 10^{-12}$$

$$T_{0,1} = 310 \quad e_0 := 1.602 \cdot 10^{-19} \quad Avo := 6.022 \cdot 10^{23}$$

There are different in radius of cell, defined as "a"

$$\begin{pmatrix} ar \\ an \\ al \end{pmatrix} := \begin{pmatrix} 3.5 \cdot 10^{-6} \\ 6 \cdot 10^{-6} \\ 5 \cdot 10^{-6} \end{pmatrix} \quad ar = 3.5 \times 10^{-6} \quad an = 6 \times 10^{-6} \quad al = 5 \times 10^{-6}$$

$$pH := 7.4$$

$$n := (10^{-pH} \cdot 10^3) \cdot Avo \quad n = 2.397 \times 10^{19} \quad n \text{ is } (10^{-pH}) \times 10^3 \times \text{Avocado No.}$$

$$z := 1 \text{ univalence}$$

Attractive force (Va) between cells and cellulose substrate

$$\begin{pmatrix} Aca \\ Ared \\ Aleu \end{pmatrix} := \begin{pmatrix} 6.7 \cdot 10^{-21} \\ 9 \cdot 10^{-21} \\ 5 \cdot 10^{-21} \end{pmatrix}$$

Aca is hamaker constant of cellulose polymer
Ared is of RBC
Alev is of Leukocytes

$$Ac := \sqrt{Aca} \quad Ac = 8.185 \times 10^{-11}$$

$$Ar := \sqrt{Ared} \quad Ar = 9.487 \times 10^{-11}$$

$$AL := \sqrt{Aleu} \quad AL = 7.071 \times 10^{-11}$$

$$A1 := Ac \cdot Ar \quad A1 = 7.765 \times 10^{-21} \quad J \quad \text{Hamaker constant between CA and RBC}$$

$$A2 := Ac \cdot AL \quad A2 = 5.788 \times 10^{-21} \quad J \quad \text{Hamaker constant between CA and WBC}$$

Variable parameters are radius of cell (a) and hamaker constant (A)

$$\text{RBC} \quad \text{Var}_i := \left(\frac{-A1}{6} \right) \cdot \left[\frac{2 \cdot ar \cdot (D_i + ar)}{D_i \cdot (D_i + 2 \cdot ar)} + \ln \left(\frac{D_i}{D_i + 2 \cdot ar} \right) \right]$$

$$\text{Neu} \quad \text{Van}_i := \left(\frac{-A2}{6} \right) \cdot \left[\frac{2 \cdot an \cdot (D_i + an)}{D_i \cdot (D_i + 2 \cdot an)} + \ln \left(\frac{D_i}{D_i + 2 \cdot an} \right) \right]$$

$$\text{Lym} \quad \text{Val}_i := \left(\frac{-A2}{6} \right) \cdot \left[\frac{2 \cdot al \cdot (D_i + al)}{D_i \cdot (D_i + 2 \cdot al)} + \ln \left(\frac{D_i}{D_i + 2 \cdot al} \right) \right]$$

zeta potential at different temperatures and repulsive force estimation

for j := 0..1

particles	298K	310K	
$\begin{pmatrix} \text{CA} \\ \text{CTA} \end{pmatrix}$	zeta_p := $\begin{pmatrix} -0.068 & -0.0667 \\ -0.0784 & -0.0758 \end{pmatrix}$		$\begin{pmatrix} 0,0 & 0,1 \\ 1,0 & 1,1 \end{pmatrix}$

$\begin{pmatrix} \text{RBC} \\ \text{Lym} \\ \text{Neu} \end{pmatrix}$	zeta_cell := $\begin{pmatrix} -0.0744 & -0.0730 \\ -0.0655 & -0.0630 \\ -0.0627 & -0.0608 \end{pmatrix}$		$\begin{pmatrix} 0,0 & 0,1 \\ 1,0 & 1,1 \\ 2,0 & 2,1 \end{pmatrix}$
--	--	--	---

$$\kappa_{0,j} := \sqrt{\frac{e0^2 \cdot n \cdot z^2}{\epsilon0 \cdot \epsilonp \cdot k \cdot T_{0,j}}} 10^{-2}$$

a. CA-RBC at 298K (j=0) and 310K (j=1)

$$V_{rr, j} := \pi \cdot \epsilon_p \cdot \epsilon_0 \cdot \text{ar} \cdot \left[\left[(\text{zeta}_{p0, j})^2 + (\text{zeta}_{\text{cell}0, j})^2 \right] \cdot \ln \left(\frac{e^{2 \cdot \kappa_{0, j} \cdot D_i} - 1}{e^{2 \cdot \kappa_{0, j} \cdot D_i}} \right) + (2 \cdot \text{zeta}_{p0, j} \cdot \text{zeta}_{\text{cell}0, j}) \cdot \ln \left(\frac{e^{\kappa_{0, j} \cdot D_i} + 1}{e^{\kappa_{0, j} \cdot D_i} - 1} \right) \right]$$

b. CA-Lym at 298K (j=0) and 310K (j=1)

$$V_{rl, j} := \pi \cdot \epsilon_p \cdot \epsilon_0 \cdot \text{al} \cdot \left[\left[(\text{zeta}_{p0, j})^2 + (\text{zeta}_{\text{cell}1, j})^2 \right] \cdot \ln \left(\frac{e^{2 \cdot \kappa_{0, j} \cdot D_i} - 1}{e^{2 \cdot \kappa_{0, j} \cdot D_i}} \right) + (2 \cdot \text{zeta}_{p0, j} \cdot \text{zeta}_{\text{cell}1, j}) \cdot \ln \left(\frac{e^{\kappa_{0, j} \cdot D_i} + 1}{e^{\kappa_{0, j} \cdot D_i} - 1} \right) \right]$$

c. CA -Neu at 298K (j=0) and 310K (j=1)

$$V_{m, j} := \pi \cdot \epsilon_p \cdot \epsilon_0 \cdot \text{an} \cdot \left[\left[(\text{zeta}_{p0, j})^2 + (\text{zeta}_{\text{cell}2, j})^2 \right] \cdot \ln \left(\frac{e^{2 \cdot \kappa_{0, j} \cdot D_i} - 1}{e^{2 \cdot \kappa_{0, j} \cdot D_i}} \right) + (2 \cdot \text{zeta}_{p0, j} \cdot \text{zeta}_{\text{cell}2, j}) \cdot \ln \left(\frac{e^{\kappa_{0, j} \cdot D_i} + 1}{e^{\kappa_{0, j} \cdot D_i} - 1} \right) \right]$$

d. CTA-RBC at 298K (j=0) and 310K (j=1)

$$V_{rr, j} := \pi \cdot \epsilon_p \cdot \epsilon_0 \cdot \text{ar} \cdot \left[\left[(\text{zeta}_{p1, j})^2 + (\text{zeta}_{\text{cell}0, j})^2 \right] \cdot \ln \left(\frac{e^{2 \cdot \kappa_{0, j} \cdot D_i} - 1}{e^{2 \cdot \kappa_{0, j} \cdot D_i}} \right) + (2 \cdot \text{zeta}_{p1, j} \cdot \text{zeta}_{\text{cell}0, j}) \cdot \ln \left(\frac{e^{\kappa_{0, j} \cdot D_i} + 1}{e^{\kappa_{0, j} \cdot D_i} - 1} \right) \right]$$

e. CTA-Lym at 298K (j=0) and 310K (j=1)

$$V_{rl, j} := \pi \cdot \epsilon_p \cdot \epsilon_0 \cdot \text{al} \cdot \left[\left[(\text{zeta}_{p1, j})^2 + (\text{zeta}_{\text{cell}1, j})^2 \right] \cdot \ln \left(\frac{e^{2 \cdot \kappa_{0, j} \cdot D_i} - 1}{e^{2 \cdot \kappa_{0, j} \cdot D_i}} \right) + (2 \cdot \text{zeta}_{p1, j} \cdot \text{zeta}_{\text{cell}1, j}) \cdot \ln \left(\frac{e^{\kappa_{0, j} \cdot D_i} + 1}{e^{\kappa_{0, j} \cdot D_i} - 1} \right) \right]$$

f. CTA -Neu at 298K (j=0) and 310K (j=1)

$$V_{rn, j} := \pi \cdot \epsilon_p \cdot \epsilon_0 \cdot \text{an} \cdot \left[\left[(\text{zeta}_{p1, j})^2 + (\text{zeta}_{\text{cell}2, j})^2 \right] \cdot \ln \left(\frac{e^{2 \cdot \kappa_{0, j} \cdot D_i} - 1}{e^{2 \cdot \kappa_{0, j} \cdot D_i}} \right) + (2 \cdot \text{zeta}_{p1, j} \cdot \text{zeta}_{\text{cell}2, j}) \cdot \ln \left(\frac{e^{\kappa_{0, j} \cdot D_i} + 1}{e^{\kappa_{0, j} \cdot D_i} - 1} \right) \right]$$

Net interaction force (F) calculated from summary force of attractive force and repulsive force

$$F_{cn,i,j} := V_{an,i} + V_{rn,i,j}$$

$$F_{ctr,i,j} := V_{ar,i} + V_{rtr,i,j}$$

$$F_{cl,i,j} := V_{al,i} + V_{rl,i,j}$$

$$F_{cl,i,j} := V_{al,i} + V_{rl,i,j}$$

$$F_{ctn,i,j} := V_{an,i} + V_{rtn,i,j}$$

$$F_{cr,i,j} := V_{ar,i} + V_{rr,i,j}$$

APPENDIX B

RESULTS OF INTERACTION FORCE ESTIMATION BY DLVO THEORY

In case of same radius (radius = 6 μm)

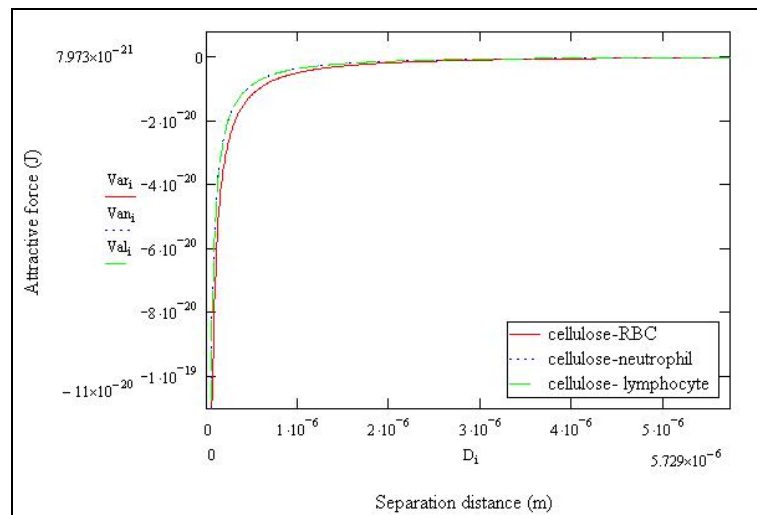


Figure B1 The attractive force between cellulose substrate and human blood cells in case of same radius ($a = 6 \times 10^{-6}$ m)

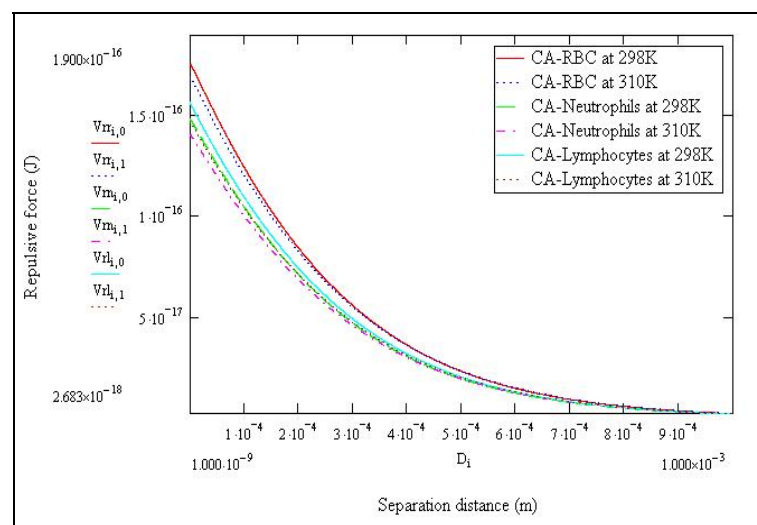


Figure B2 The repulsive force between each cells type and CA substrate at 298K and 310K in case of same radius ($a = 6 \times 10^{-6}$ m)

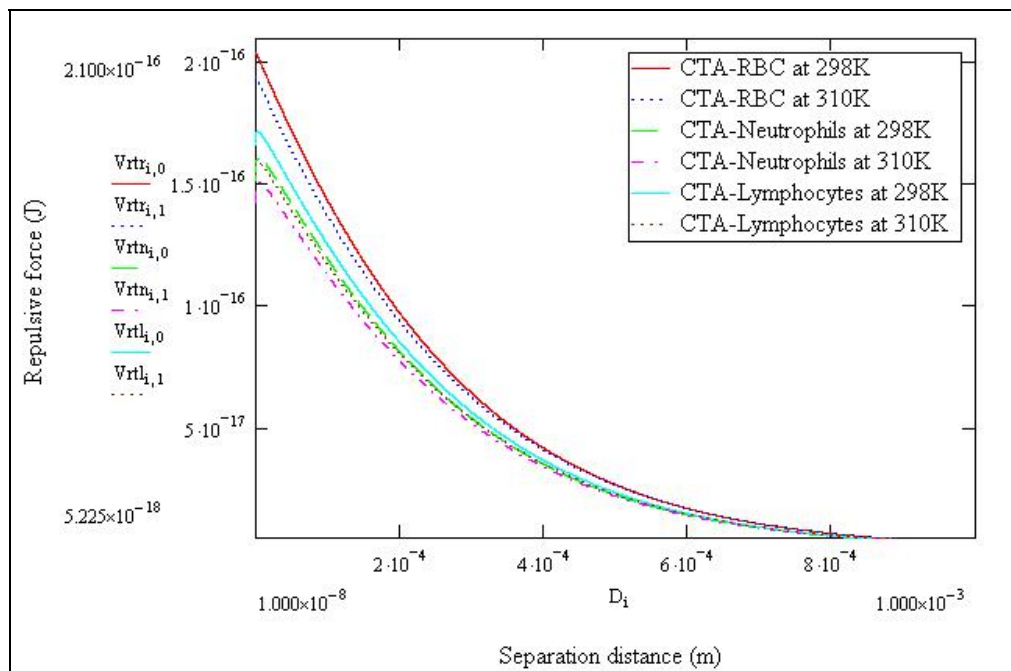


Figure B3 The repulsive force between each cells type and CTA substrate at 298 and 310K in case of same radius ($a = 6 \times 10^{-6}$ m)

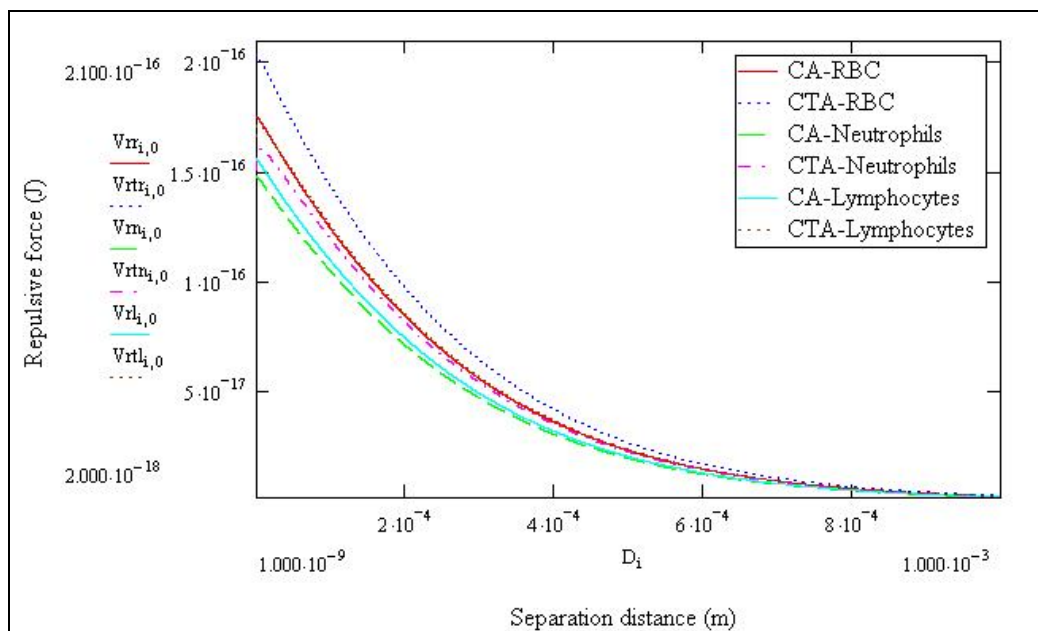


Figure B4 The repulsive force between each cells type and each substrate at 298K in case of same radius ($a = 6 \times 10^{-6}$ m)

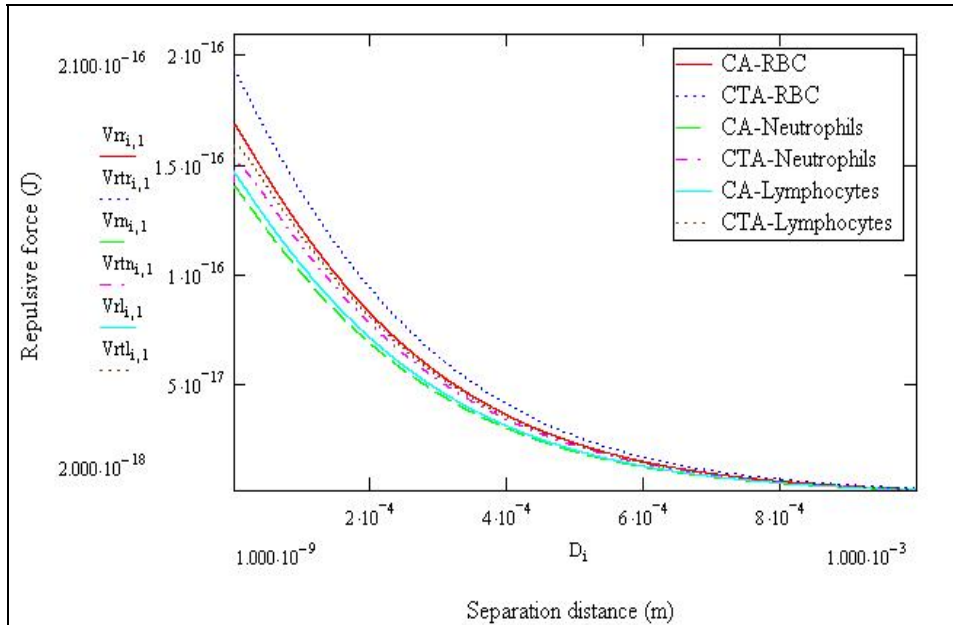


Figure B5 The repulsive force between each cells type and each substrate at 310K in case of same radius ($a = 6 \times 10^{-6}$ m)

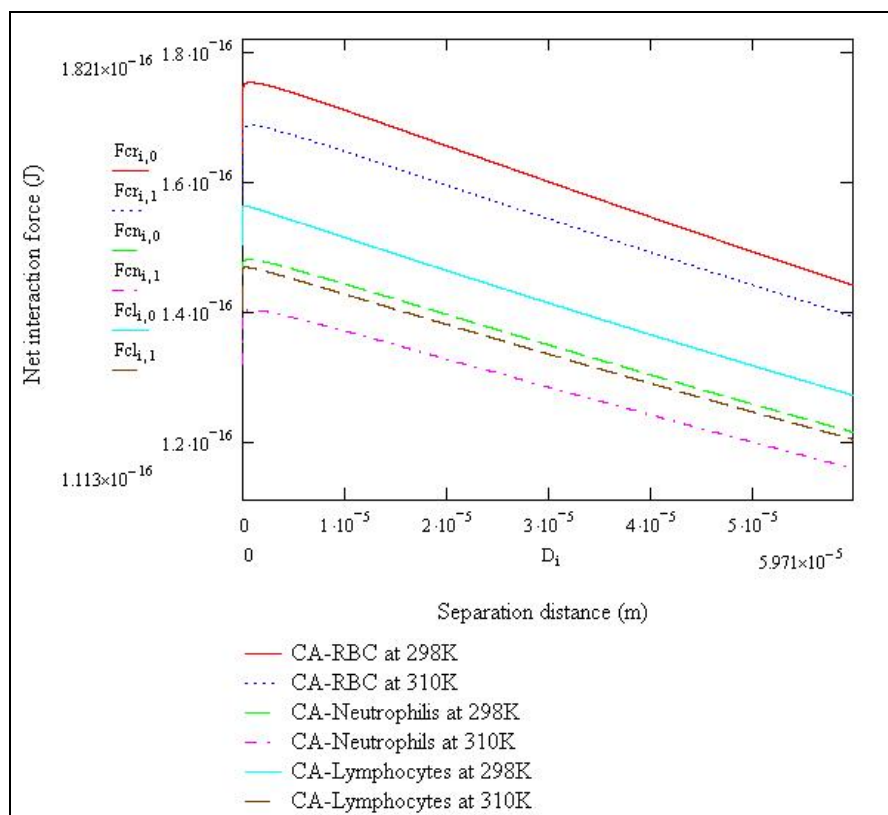


Figure B6 The net interaction force between CA and each blood cell type at 289K and 310K in case of same radius ($a = 6 \times 10^{-6}$ m)

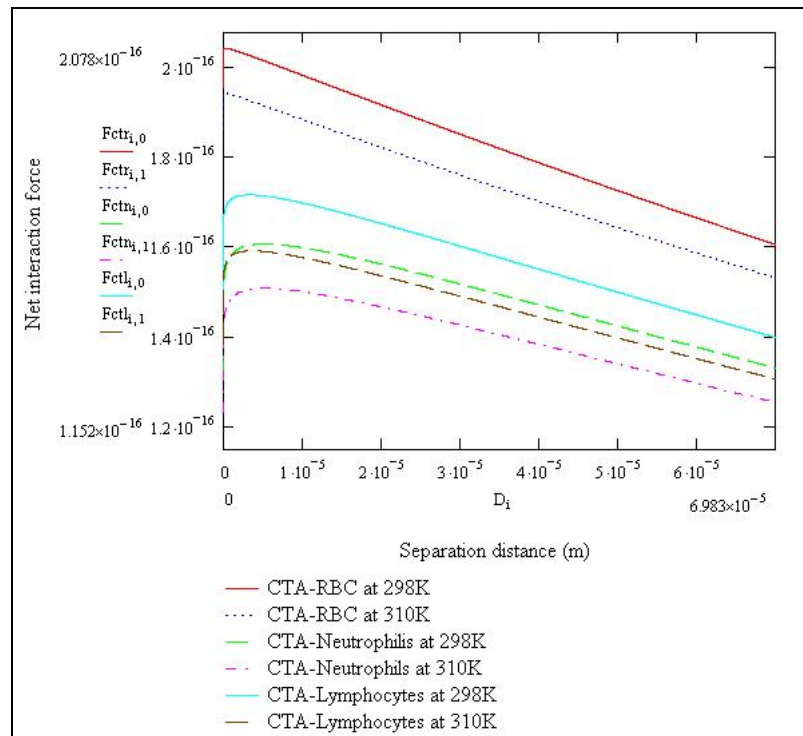


Figure B7 The net interaction force between CTA and each blood cell type at 289K and 310K in case of same radius ($a = 6 \times 10^{-6}$ m)

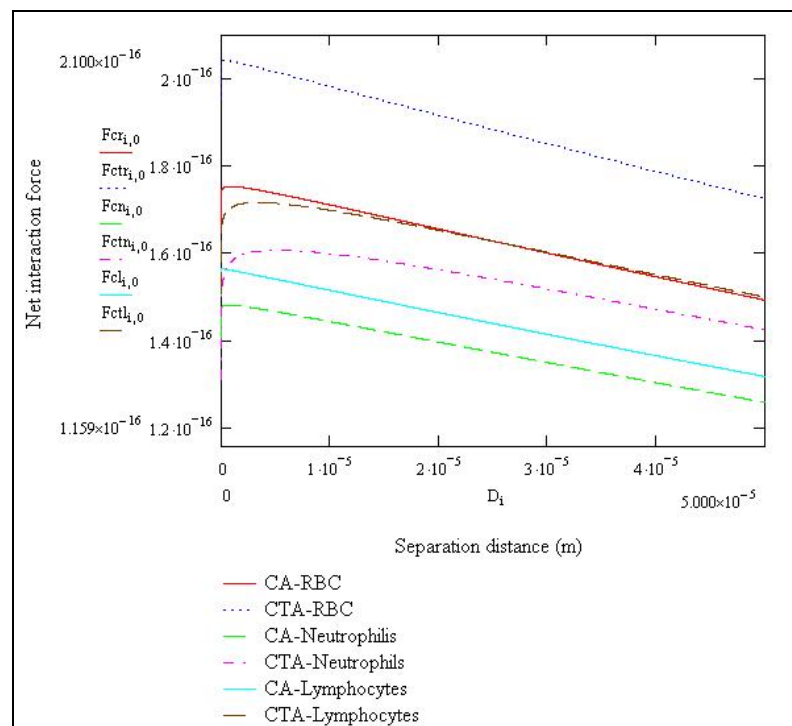


Figure B8 The net interaction force between each substrate and each blood cell type at 298K temperatures in case of same radius ($a = 6 \times 10^{-6}$ m)

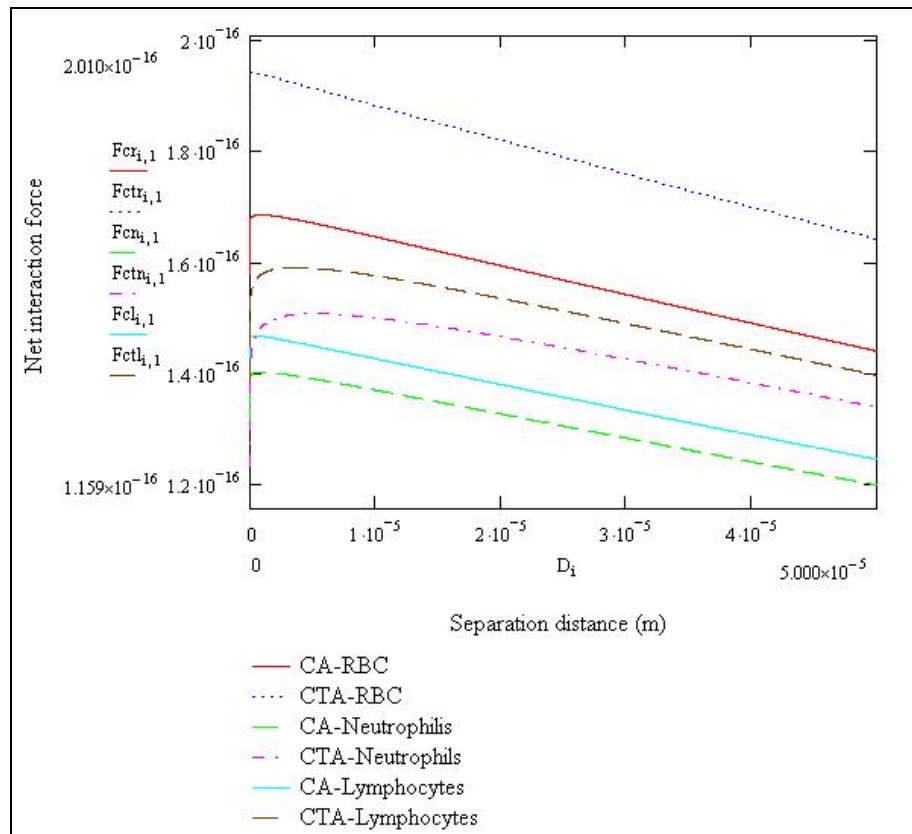


Figure B9 The net interaction force between each substrate and each blood cell type at 310K temperatures in case of same radius ($a = 6 \times 10^{-6}$ m)

APPENDIX C
CELLULOSE SUBSTRATES PREPARATION COMPOSITIONS

Table C1 Compositions of film samples (% w/v)

Sample ID	Cellulose acetate (g)	Cellulose triacetate (g)	Chloroform (ml)	Methanol (ml)	Acetone (ml)
CA5	0.25	-	-	-	10
CTA5	-	0.25	9	1	-
CA10	0.5	-	-	-	10
CTA10	-	0.5	9	1	-

APPENDIX D

ZETA POTENTIAL OF VARIOUS CELLULOSE POLYMERS

AND VARIOUS BLOOD CELL TYPES

Table D1 Zeta potential measurement of blood cell and polymer in 5%PVP solution at 298 K and 310 K (n=3)

Sample ID	Samples	Temperature (K)	Trial			Mean (\bar{x})	SD
			1	2	3		
CA298K	Cellulose acetate	298	-68.9	-68.2	-66.7	-68.0	1.2
CA310K	Cellulose triacetate	310	-66.9	-66.2	-67.1	-66.7	0.5
CTA298K	Cellulose acetate	298	-78.6	-76.8	-79.7	-78.4	1.5
CTA310K	Cellulose triacetate	310	-76.1	-73.7	-77.7	-75.8	2.0
RBC298K	Red blood cell	298	-70.7	-75.1	-77.5	-74.4	3.4
RBC310K	Red blood cell	310	-72.6	-74.5	-71.9	-73.0	1.3
LYM298K	Lymphocyte	298	-65.5	-67.2	-63.7	-65.5	1.8
LYM310K	Lymphocyte	310	-63.9	-63.7	-61.3	-63.3	1.4
NEU298K	Neutrophil	298	-63.7	-63.9	-60.6	-62.7	1.8
NEU310K	Neutrophil	310	-61.5	-61.7	59.1	60.8	1.4

APPENDIX E
ENERGY BARRIER FROM NET INTERACTION FORCE
BETWEEN CELLS AND SUBSTRATES

Table E1 Maximum net energy barrier between blood cell and CA or CTA substrate at 298 K and 310 K, in case of various cell radiuses

Sample ID	Substrate	Type of cell	Energy barrier (J)	
			298K	310K
CA-RBC	CA	Red blood cell	1.023E-16	9.84E-17
CA-Neutrophil	CA	Neutrophil	1.481E-16	1.404E-16
CA-Lymphocyte	CA	Lymphocyte	1.303E-16	1.224E-16
CTA-RBC	CTA	Red blood cell	1.191E-16	1.133E-16
CTA-Neutrophil	CTA	Neutrophil	1.607E-16	1.509E-16
CTA-Lymphocyte	CTA	Lymphocyte	1.43E-16	1.327E-16

Table E2 Maximum net energy barrier between blood cell and CA or CTA substrate at 298 K and 310 K, in case of same cell radius (radius = 6 μm)

Sample ID	Substrate	Type of cell	Energy barrier (J)	
			298K	310K
CA-RBC	CA	Red blood cell	1.753E-16	1.687E-16
CA-Neutrophil	CA	Neutrophil	1.481E-16	1.404E-16
CA-Lymphocyte	CA	Lymphocyte	1.564E-16	1.469E-16
CTA-RBC	CTA	Red blood cell	2.042E-16	1.943E-16
CTA-Neutrophil	CTA	Neutrophil	1.607E-16	1.509E-16
CTA-Lymphocyte	CTA	Lymphocyte	1.716E-16	1.592E-16

APPENDIX F**NUMBER OF BLOOD CELLS ON CELLULOSE SUBSTRATES****Table F1** The number of blood cells ($\times 10^6$ cells/ mm^2) adhered on substrate at 298 K and 310 K for 1, 2 and 3 hour incubation time (n=3)

Sample ID	Incubation time (h)	Trial			Mean (\bar{x})	SD
		1	2	3		
CA10-1H	1	0.0894	0.0921	0.0867	0.0894	0.0027
CA5-2H	2	0.1143	0.1111	0.1056	0.1103	0.0043
CA5-3H	3	0.1327	0.1327	0.1295	0.1317	0.0018
CA10-1H	1	0.0298	0.0135	0.0208	0.0214	0.0081
CA10-2H	2	0.0460	0.0298	0.0325	0.0361	0.0087
CA10-3H	3	0.0840	0.0677	0.0785	0.0767	0.0082
CTA5-1H	1	0.0027	0.0108	0.0162	0.0099	0.0068
CTA5-2H	2	0.0108	0.0189	0.0271	0.0189	0.0081
CTA5-3H	3	0.0135	0.0216	0.0325	0.0225	0.0095
CTA10-1H	1	0.0027	0.0054	0.0054	0.0045	0.0015
CTA10-2H	2	0.0135	0.0081	0.0108	0.0108	0.0027
CTA10-3H	3	0.0135	0.0189	0.0162	0.0162	0.0027

Table F2 The number of neutrophils ($\times 10^6$ cells/ mm^2) adhered on substrate at 298 K and 310 K for 1, 2 and 3 hour incubation time (n=3)

Sample ID	Incubation time (h)	Trial			Mean (\bar{x})	SD
		1	2	3		
CA10-1H	1	0.0626	0.0742	0.0715	0.0694	0.0060
CA5-2H	2	0.0888	0.0977	0.0888	0.0918	0.0051
CA5-3H	3	0.1062	0.1181	0.1062	0.1102	0.0069
CA10-1H	1	0.0195	0.0166	0.0195	0.0185	0.0016
CA10-2H	2	0.0246	0.0246	0.0281	0.0258	0.0020
CA10-3H	3	0.0607	0.0607	0.0607	0.0607	0
CTA5-1H	1	0.0108	0.0108	0.0108	0.0108	0
CTA5-2H	2	0.0189	0.0189	0.0189	0.0189	0
CTA5-3H	3	0.0216	0.0216	0.0216	0.0216	0
CTA10-1H	1	0.0048	0.0048	0.0054	0.0050	0.0003
CTA10-2H	2	0.0108	0.0108	0.0108	0.0108	0
CTA10-3H	3	0.0162	0.0162	0.0146	0.0157	0.0009

Table F3 The number of lymphocytes ($\times 10^6$ cells/ mm^2) adhered on substrate at 298 K and 310 K for 1, 2 and 3 hour incubation time (n=3)

Sample ID	Incubation time (h)	Trial			Mean (\bar{x})	SD
		1	2	3		
CA10-1H	1	0.0178	0.0152	0.0178	0.0169	0.0015
CA5-2H	2	0.0222	0.0133	0.0222	0.0192	0.0051
CA5-3H	3	0.0265	0.0146	0.0265	0.0225	0.0069
CA10-1H	1	0.0021	0.0049	0.0021	0.0031	0.0016
CA10-2H	2	0.0105	0.0105	0.0070	0.0093	0.0020
CA10-3H	3	0.0151	0.0151	0.0151	0.0151	0
CTA5-1H	1	0	0	0	0	0
CTA5-2H	2	0	0	0	0	0
CTA5-3H	3	0	0	0	0	0
CTA10-1H	1	0.0005	0.0005	0	0.0003	0.0003
CTA10-2H	2	0	0	0	0	0
CTA10-3H	3	0	0	0.0016	0.0005	0.0009

Table F4 The number of eosinophils ($\times 10^6$ cells/ mm^2) adhered on substrate at 298 K and 310 K for 1, 2 and 3 hour incubation time (n=3)

Sample ID	Incubation time (h)	Trial			Mean (\bar{x})	SD
		1	2	3		
CA10-1H	1	0.0089	0	0	0.0029	0.0051
CA5-2H	2	0	0	0	0	0
CA5-3H	3	0	0	0	0	0
CA10-1H	1	0	0	0	0	0
CA10-2H	2	0	0	0	0	0
CA10-3H	3	0	0	0	0	0
CTA5-1H	1	0	0	0	0	0
CTA5-2H	2	0	0	0	0	0
CTA5-3H	3	0	0	0	0	0
CTA10-1H	1	0	0	0	0	0
CTA10-2H	2	0	0	0	0	0
CTA10-3H	3	0	0	0	0	0

BIOGRAPHY

NAME	Miss Thaneeya Samwang
DATE OF BIRTH	June 06, 1981
PLACE OF BIRTH	Nonthaburi, Thailand
INSTITUTIONS ATTENDED	Mahidol University, 1998-2001: Bachelor of Science (Medical technology) Mahidol University, 2002-2006: Master of Engineering (Biomedical Engineering)
HOME ADDRESS	31/2 M. 6, Thima, Muang, Nonthaburi, Thailand 11000 Tel. 08-9401-6537 E-mail: wufei05@hotmail.com, tan_775@yahoo.com